Belowground communities in lowlands are less stable to climate extremes across seasons

Gerard Martínez-De León[1, *], Ludovico Formenti[1], Jörg-Alfred Salamon[2], Madhav P. Thakur[1]

[1] *Institute of Ecology and Evolution, University of Bern, Switzerland*

[2] *Institute of Animal Ecology & Field Station Schapen, University of Veterinary Medicine Hannover, Germany*

*Corresponding author

Gerard Martínez-De León

Institute of Ecology and Evolution

Baltzerstrasse 6, CH-3012 Bern, Switzerland

Email: gerard.martinezdeleon@unibe.ch

Author Contributions: GMDL and MPT conceived the study. GMDL led the experiments and collected the data, with technical support from LF. JAS conducted the taxonomic determination of Collembola species. GMDL analyzed the data with the inputs from MPT. GMDL wrote the manuscript with substantial contributions from MPT. All authors revised and approved the final manuscript.

Keywords: Collembola, fungi, resistance, recovery, thermal vulnerability.

Abstract

Ecological responses to climate extremes vary drastically in different spatiotemporal contexts. For instance, the seasonal timing could be a major factor influencing community responses, but its importance is likely to vary at different spatial settings, such as high or low elevation. Here, we investigate how soil communities at high- and low-elevation sites respond to extreme heat events at different seasons (spring, summer and autumn). We simulated one-week heat events based on site-specific climatic history in several laboratory experiments using 360 field-collected soil cores, and measured the resistance and recovery of two major groups of soil biota: Collembola and fungi. We found that Collembola communities from low elevations showed the lowest resistance to extreme heat in spring and summer, with full recovery only observed in spring soils. However, species-specific analysis using joint species distribution models showed that cold-adapted taxa from lower elevations could not recover completely after extreme heat, suggesting range contractions due to climate extremes. Although fungal communities generally remained stable, pathogens increased and saprotrophs declined following extreme heat. Network analysis revealed that the connectance of negative associations between Collembola and fungi increased in response to extreme heat events, indicating that deleterious fungal species constrained the recovery of certain collembolan species. We provide experimental evidence for how heat events can restructure and destabilize ecological communities depending on spatiotemporal contexts like elevation and seasonal timing.

Significance Statement

As climate extremes become more frequent and severe, examining how distinct ecological settings differ in their degree of vulnerability has direct implications for our broad understanding of climate change effects on biodiversity. We experimentally exposed soil communities collected at different elevations and seasons to extreme heat events –based on site-specific climatic history- and measured the stability (resistance and recovery) of Collembola and fungi, representing key trophic groups in belowground food chains. Our results show that lowland communities responded strongly to the extreme heat events, while

highland communities remained largely unaltered. Remarkably, lowland communities recovered better in spring than in summer, underscoring the importance of the seasonal context in determining ecological stability to climate extremes.

Introduction

Contemporary climate change is causing more frequent and severe extreme heat events, with significant ecological impacts (1–3). For instance, extreme heat can push organisms beyond their adaptive capacities, exceeding physiological thermal optima and leading to declines in their performance (4, 5). Short-term vulnerability to extreme heat (i.e., resistance during and immediately after the disturbance) is determined by the magnitude of thermal change experienced by an organism (i.e., exposure) and the concomitant fitness response (i.e., sensitivity) (6–8) . It has been shown that thermal vulnerability varies across latitudinal gradients, with tropical and mid-latitude ectotherms being more susceptible to elevated temperatures. This increased vulnerability occurs because, despite having similar heat tolerances to organisms from higher latitudes (9), tropical and mid-latitude ectotherms experience temperatures closer to their thermal limits (10, 11). However, when scaling up from organismal to population and community levels, additional factors can influence thermal vulnerability (12), such as the seasonal timing of heat events (13, 14).

The ecological significance of the timing of extreme events depends on the degree of exposure of heat-sensitive life-history processes (e.g., juvenile survival (15), reproduction (16)). Consequently, the impact of extreme heat will be amplified when it coincides with key phenological periods (13, 17), with implications for long-term ecological dynamics such as population recovery (7, 18). For example, when heat extremes occur during reproductive periods, recruitment may be able to compensate for heat-induced impacts on adult survival (19), but such impacts may also persist in the long term if additional breeding attempts are no longer feasible (20) (e.g., late in the reproductive period) or if recruitment is hindered (19) (e.g., owing to reduced juvenile viability). These key phenological periods are not only seasonally dependent but also change spatially, as they are shaped by local climatic conditions (21).

Thus, given that phenology and thermal vulnerability vary across geographic gradients (12, 21), the ecological consequences of extreme heat events could differ depending on both the seasonal timing and the geographical context. Yet, these important spatial and temporal ecological dimensions (i.e., geography and seasonal timing) have rarely been considered in comparative studies of thermal vulnerability, despite their potential to interactively influence short- and long-term ecological stability to extreme heat events.

Elevational gradients provide unique opportunities to examine variation in ecological responses to temperature changes (22), including extreme heat events. Local climatic conditions vary radically over short distances across elevations as a result of temperature lapse rates (23), and, in many temperate environments, due to orographic precipitation (24). These abiotic factors are main drivers of phenology at the site scale (17), and thereby generate variation in phenological patterns across elevations (24). For instance, in temperate ecosystems, organisms living at high elevation sites have typically short activity periods condensed around the summer months (17, 24). In turn, organisms inhabiting low elevation sites have generally longer activity periods, only interrupted in dry summers and in the winter months. These distinct phenological patterns may underlie distinct periods of high thermal vulnerability and, therefore, the seasonal timing of extreme heat events is expected to exert distinct impacts across elevations. For example, at low elevations, very hot conditions during the summer months can have significant impacts on survival (25). However, avoidance strategies commonly displayed by low-elevation organisms, such as seasonal escape or induced diapause, may enable them to evade the harsh effects of extreme heat (26, 27) . At higher elevations, summer is typically a favorable period for reproduction and recruitment in many species, but these processes could be compromised if temperatures during extreme heat events exceed the thermal limits for fertility or embryo viability (16, 28).

Within a given community, there is enormous variation across different taxa in their life-histories and thermal responsiveness (29, 30), potentially leading to trophic mismatches after extreme heat events (31, 32). In belowground or soil communities, fungi are key drivers of ecosystem functioning (33) and represent important resources for many invertebrate consumers, especially for microbivores such as

Collembola (34, 35). Fungi form the foundation of the slow energy channel in soil food webs (36, 37). Consequently, fungal communities are often highly resistant to climate extremes (e.g., heat (38) and drought (39)), although they tend to recover slowly after disturbances (40). Given the overall stability of fungal communities to climate extremes, they can represent readily available resources for recovering populations of invertebrate consumers like Collembola, thereby promoting overall food web stability (41). However, increasing severity of climate extremes could affect fungal responses in the long term (38, 42), constraining the recovery of invertebrate consumers. In addition, climate-driven shifts in fungal communities could also result in increased dominance of fungal species that represent poor-quality resources (because of e.g., low palatability or nutritional value) (43) or even pathogens (44), further limiting the recovery of soil Collembola. The structure of association networks between Collembola and fungi can therefore yield additional insights into their responses to extreme heat events. Specifically, more prevalent positive associations between Collembola and fungi in recovering communities after extreme heat (i.e., more connectance, indicating more generalized associations) (45, 46) can be expected, as Collembola might become more reliant on fungal resources to sustain their populations. Correspondingly, negative Collembola-fungal associations could also become more frequent during the recovery after extreme heat, as a result of climate-driven increases of fungi representing low-quality resources and/or pathogenic species (43), thus limiting the recovery of Collembola species.

Here, we investigated how belowground communities respond to extreme heat events, using intact soil cores collected from temperate grasslands at two different elevations (spanning ~1000 m of altitude difference) and across three seasons (spring, summer, autumn) (Fig. 1). We exposed these field-collected soil cores to one-week extreme heat events in controlled laboratory conditions, and tracked the responses of two trophic levels (Collembola and fungi) at the end of extreme heat (i.e., resistance response) and after a five-week recovery period (i.e., recovery response) -representing the generation time of several Collembola species. We examined how the extreme heat events altered total abundances, species-specific abundances (using joint species distribution models), diversity indices (calculated via Hill numbers), and bipartite association networks of Collembola and fungi (focusing on connectance and network dissimilarity). Our hypotheses are (1) that heat events reaching higher temperatures (e.g., low

elevation sites in summer) will induce more negative responses, given that the thermal safety margins of organisms are narrower (i.e. closer to their thermal limits) and metabolic costs are greater at high absolute temperatures (10, 47). Moreover, we expect that (2) negative resistance responses, driven by heat-induced mortality, will be followed by negative recovery responses, primarily influenced by recruitment following the extreme heat event in closed populations. This will apply mainly to cold-adapted organisms, due to their lower heat tolerance or reduced performance at high temperatures (18), and those permanently living belowground, given their greater sensitivity to thermal variation (48, 49). We finally anticipate (3) heat-induced shifts in the structure of association networks between Collembola and fungi, resulting in higher connectance of positive (46) (indicating increased reliance of Collembola on a broader range of fungal resources) and/or negative (43) associations (indicative of greater limitation of Collembola by low-quality resources or pathogens).

Results

Collembola communities: total abundance and diversity responses

Collembola abundance and diversity were affected by extreme heat at low elevation in spring and summer, while the effects in autumn and at high elevation (across seasons) were negligible (Fig. 2; Fig. S6). At low elevation sites, Collembola abundance dropped in spring (-69%) and summer (-77%) at the resistance phase. Remarkably, Collembola abundance at low elevation recovered completely in spring, but significant deviations from control treatments (i.e., negative recovery) persisted in summer (-76%; Fig. 2, Table S9). Diversity metrics mirrored the responses of Collembola abundance in spring at low elevation (i.e., negative resistance in all diversity metrics, e.g., -49% Shannon-Hill; followed by complete recovery), but not in summer, since diversity metrics were not affected by extreme heat in this case (Fig. S6). Negative recovery responses of Shannon-Hill and Simpson-Hill diversity were also observed at high elevation in autumn, although the magnitude of such responses was less notable (-23% Shannon Hill and -26% Simpson-Hill compared to control treatment; Fig. S6).

Collembola communities: species-specific abundance responses

Out of the nine Collembola species included in the analysis of species abundances (see Methods for the inclusion criteria), eight species showed negative responses in spring at our low elevation sites at the resistance phase (Fig. 3a). Later, most of them attained a complete recovery (6 out of 9), except for *Protaphorura pseudovanderdrifti, Isotomiella minor* and *Lepidocyrtus cyaneus* (Fig. 3b). Even though these species occurred at both elevations, they were significantly lesser abundant at low elevation sites (Fig. 3; Fig. S7). The mean proportion of raw variance in species abundances explained by extreme heat increased from the baseline (pseudo-R^2 = 0.05) to the resistance phase (pseudo-R^2 = 0.10), and was then maintained at the recovery phase (pseudo-R^2 = 0.09; Fig. 3). Besides, we found that the vertical stratification across the soil profile of Collembola species did not explain changes in species abundances driven by extreme heat (Fig. S8).

Fungal communities

Fungal communities generally remained stable in response to the extreme heat events across elevations and seasons, as extreme heat did not alter either fungal diversity (Fig. S9) or, in general terms, the occurrences and abundances of fungal species (Figs. S10-12). However, various fungal trophic groups responded to extreme heat in the recovery response: total saprotroph reads declined in autumn (-34%) (Fig. 4a) and non-significantly in spring and in summer at low elevation (Table S10), whereas pathogen reads increased markedly in summer at low elevation (+129%) (Fig. 4b; Table S11). Besides, total reads of unassigned fungi increased (+28%), while those of symbiotic fungi declined (-61%) in autumn at low elevation (Fig. S14). The occurrences of several pathogens exposed to extreme heat were higher at the recovery response (mainly in spring at low elevation, and in summer at high elevation; Fig. S13), but not their species abundances (Fig. S12).

Collembola-fungal association networks at the recovery response

Extreme heat altered the connectance of Collembola-fungal association networks in recovering communities from low elevation in spring (Fig. 5; Table S12). Compared to random expectations from null models, the connectance of negative associations increased in networks exposed to extreme heat events (connectance difference: 0.075; $P = 0.003$) (Fig. 5; Table S12). This rise in network connectance was driven by a higher number of negative associations between Collembola and saprotrophic fungi species (Table S12). Moreover, we observed that the dissimilarity between control and extreme heat networks from low elevation in spring was primarily determined by compositional effects, with species composition accounting for 65% of network dissimilarity (Table S12). This indicates that a distinct set of species contributed to the assembly of association networks during the recovery period (Fig. S15).

Discussion

We found that belowground communities responded differently to experimental extreme heat events across elevations and seasons, as well as depending on the trophic level. Collembolan communities were especially more susceptible to extreme heat events at low elevations, confirming our initial expectations. However, recovery was season-dependent at low elevations, as collembolan communities managed to compensate previous heat-induced declines in spring but not in summer, further suggesting that collembolans from summer soils in lowlands were the most vulnerable ones. Fungal communities were in general stable to extreme heat events, with some marked exceptions for fungal saprotroph and pathogen species, also notably so at low elevations. Our results further revealed that extreme heat altered the structure of Collembola-fungal associations in recovering lowland communities, mainly by increasing the connectance of negative associations in spring.

Extreme heat events caused stronger ecological effects on low elevation communities

Low elevation belowground communities were disproportionally impacted by extreme heat compared to those at high elevation, particularly the collembolan communities. This finding supports the known geographic patterns of thermal vulnerability across latitudinal gradients (12), demonstrating that organisms currently experiencing warm conditions or occasional hot periods (e.g., at low elevations) are prone to greater physiological and metabolic costs with further warming (10, 11, 47). In turn, organisms at high elevations tend to have wider thermal safety limits because their heat tolerances remain constant across elevations (50). This pattern might be explained by a lack of local adaptation in widely-distributed temperate species (9, 51), or alternatively, by high heat tolerances that enable highland organisms to cope with radiation-driven thermal extremes common in these environments (52, 53). Even though the abundances of Collembola at higher elevations remained unaltered by extreme heat, some typical highland species were particularly impacted when they also occurred at lower elevations. For example, *Protaphorura pseudovanderdrifti* showed negative resistance and recovery responses to spring heat events, and *Lepidocyrtus cyaneus* displayed negative recovery in summer. Such negative recovery responses are likely explained by the deleterious impacts of heat on fecundity, as previously showed in laboratory populations of *P. pseudovanderdrifti* (18). These findings suggest the (elevational) range contraction of typical high-elevation species in response to extreme heat events, especially as warm-adapted species may recover better and therefore exclude other species closer to their thermal niche limits (54). Importantly, heat extremes of similar severity to those simulated in our experiment are already taking place occasionally (Table S8), underscoring the relevance of our findings for natural communities in the face of present-day and future heat extremes. One limitation of our results is that greater responsiveness in certain collembolan communities may have been explained by the lack of possibilities to behaviorally thermoregulate by moving deeper in the soil (50, 55), given the depth of our soil cores. However, this limitation should not alter qualitatively our main insight, that is, that soil communities are more susceptible to extreme heat events at lower elevations, especially for species at the edge of their thermal niches.

We also found that fungal communities remained generally unaltered in response to the experimental heat events. Given that soil fungi utilize nutrients relatively slowly, they represent the slow

energy channel within soil microbial communities, which could help them to buffer pulse disturbances and increase their resistance to climate extremes (41). Indeed, it has been previously shown that many soil fungal communities are generally robust to extreme heat and drought (38, 39, 56), partly because water and nutrients can be redistributed from different parts of the fungal mycelium (57). Nonetheless, certain trophic groups from low elevation fungal communities (i.e., saprotrophs and pathogens) responded strongly to the extreme heat events, mainly in the recovery response. In particular, saprotrophic fungi reacted negatively to extreme heat after the recovery phase in autumn, and similar non-significant trends were observed in spring and summer (Fig. 4a; Table S10). These findings are consistent with their global distribution patterns, as saprotrophs are more abundant in cold and wet regions with high soil carbon content (59). In contrast, fungal pathogens became much more abundant with extreme heat after the recovery phase in summer (Fig. 4b; Table S11), partly because of increased occurrences of pathogen species (Figs. S12-13), corroborating previous findings that hotter conditions promote fungal pathogens at the global scale (44).

Seasonal-dependent effects of extreme heat on low elevation communities

Extreme heat events had distinct effects on low elevation collembolan communities depending on whether they occurred in spring or summer. In these seasons, extreme heat generally affected collembolan survival, as revealed by their negative resistance responses. Remarkably, this was followed by a complete recovery of the abundances of most species in spring, indicating that their recruitment managed to compensate for the previous heat-induced mortality. Those individuals that survived the heat event may have benefited from reduced competition, allowing for a higher fecundity and/or enhanced juvenile viability during the recovery period. By contrast, recovery remained incomplete in the summer season. We suspect that most species used a strategy of seasonal escape (26), which implies that recruitment was possibly delayed until the end of a summer diapause period (60, 61). The influence of pathogens might additionally explain the limited recovery of Collembola in summer, given that pathogenic fungi became more abundant in heat-exposed soils (Fig. 4), and were therefore more likely to infect

Collembola hosts (62). However, this possibility remains unclear, given that Collembola can exhibit high tolerance to various entomopathogenic fungi found in soils (63).

In autumn, resistance and recovery responses to extreme heat events were generally negligible, or even positive at low elevation in some Collembola species (Fig. 3). As opposed to spring and summer, ecological responses to extreme heat in autumn are likely delayed for a much longer period than the recovery phase used in our study. Many species enter a period of reduced activity or complete dormancy before the onset of winter (61), especially at high elevations. During this period, non-active individuals need to endure metabolic costs that can become even greater during extreme heat events, leading to reduced survival after the winter diapause (64). It is thus plausible that our recovery responses could not capture the deleterious effects of autumn extreme heat events, which would require the measurement of post-winter or multiyear effects in controlled experiments (e.g., (65)).

Extreme heat increased the connectance of Collembola-fungal association networks

We show that extreme heat events induced higher connectance of negative associations between Collembola and fungi in recovering communities at low elevation, mostly in spring. While these associations mainly capture the statistical signature of the relationships between collembolan and fungal abundances and not the realized feeding interactions (as in e.g., (62)), the observed shifts in association network properties can have plausible implications for the functioning of soil communities under extreme heat. As discussed above, low elevation communities were severely impacted after being exposed to spring heat events –especially so for Collembola-, but their species composition was mostly restored during the recovery period in our experiment. However, we show that alterations in the structural properties of Collembola-fungal networks persisted at the recovery response, possibly as a result of the restructuring of the communities after extreme heat events. Our results suggest that locally abundant saprotrophic fungi, possibly representing poor-quality resources, constrained the recovery of certain Collembola species, resulting in the observed pattern of increased connectance of negative Collembola-fungal associations. This occurred even if saprotrophs remained constant or even declined in response to

extreme heat. In addition, we show that the network dissimilarity between temperature treatments was largely driven by compositional effects (Table S12), which implies that increased connectance in networks from extreme heat soils might involve associations with a different set of species compared to networks in control soils. These findings confirm our hypothesis of increased heat-induced connectance of negative associations, but we did not observe higher connectance of positive associations as we also anticipated. We suggest that, as a result of temperature effects on feeding rates (66), collembolans should have more generalized (46) or stronger interactions with fungi, especially in spatiotemporal settings characterized by cooler conditions, such as at higher elevations. Further studies evaluating realized feeding interactions or food web responses during and after heat events, as previously done in freshwater systems (67), will be needed to verify this expectation in belowground communities.

To conclude, the findings from our comparative experiment, testing the impacts of extreme heat events in distinct spatiotemporal contexts (i.e., different elevations and seasons), corroborate that lowland communities are disproportionally sensitive to extreme heat, with stronger effects on invertebrate consumers (Collembola) than on their microbial resources (fungi), in line with the trophic mismatch hypothesis. Notably, collembolan communities managed to recover in spring but not in summer, which emphasizes the importance of phenological processes in determining recovery after pulse disturbances like heat extremes. Despite the general stability of fungal communities, heat-induced shifts in the relative abundances of certain trophic groups could have cascading effects on other ecological processes (e.g., infection prevalence, decomposition of organic matter), especially if these changes prevail over longer timescales. Our study illustrates how depicting resistance and recovery to heat extremes in different spatiotemporal contexts (e.g., elevation and seasons) and across trophic groups can contribute to draw a more complete picture of ecological stability in a changing world.

Materials and Methods

Field sites and experimental design

The study area was located in the Swiss Jura Mountains, consisting of two blocks (regions) located ca. 40 km apart (Fig. S1). Each block had two sites at contrasting elevations: low (ca. 500 m.a.s.l.) and high elevation (ca. 1550 m.a.s.l.) (Fig. 1.; Figs. S1-2). The climate in the study area is temperate continental, with low elevations characterized by average yearly temperatures of 10.7 °C (monthly average of the coldest and warmest month: 1.8 °C and 20.1 °C, respectively) and 956 mm of annual precipitation (based on the weather station at 485 m.a.s.l.; Table S3). At high elevations, the average yearly temperature is 4.3 °C (monthly average of the coldest and warmest months: −2.8 °C and 12.1 °C, respectively) with 1396 mm of annual precipitation (based on the weather station at 1594 m.a.s.l.; Table S3). All sites were located in extensively managed dry meadows representative of the study area, on south-facing slopes and with no recent soil disturbances (Table S1). The vegetation at high elevation sites was generally dominated by *Agrostis capillaris, Carex nigra* and *Carex montana*, while at low elevations *Bromus erectus, Trisetum flavescens* and *Securigera varia* were most abundant (Table S1). We monitored soil temperatures (at 5 cm depth) at 30-min intervals throughout the duration of the study (6 May – 9 November 2022) using data loggers (HOBO Pendant® MX, Onset Computer Corporation, USA), and retrieved mean, minimum, and maximum daily temperatures at each of the study sites (Fig. S4).

Our experimental units were intact soil cores (diameter 4.8 cm, depth 5.5 cm; Vienna Scientific Instruments, Austria) obtained in 2022 at three different seasons: spring (6-9 May), summer (4-7 July) and autumn (13-16 September). We used a split-plot experimental design (68), composed by three grouping factors (block, site and plot), as well as predictors at the site level (elevation), at the plot level (season), and at the sample level (temperature regime and harvest (69)) (Fig. 1). Within each site and season, we sampled five plots of 1.5 m x 1 m. We collected six soil cores from each plot, and randomly allocated them to the experimental treatments: one of the two temperature treatments (control conditions vs. extreme heat; details in Temperature treatments), and one of the three destructive harvests (details in Data collection). We therefore established a total of 360 experimental units: 2 elevations x 2 sites (nested

within elevation) x 3 seasons x 5 plots (nested within season) x 2 temperature treatments x 3 harvests. With this sampling design, we aimed to capture large-scale variation in the composition of soil communities from different sites, hence enhancing the generality of our study, while minimizing small-scale variation by sampling all experimental treatment combinations within the same plot (Fig. 1).

Before all soil cores were sampled, we cut the vegetation at 5 cm from the ground level to avoid overcrowding when soil cores were later incubated in the laboratory. Immediately after collecting the soil cores, we stored them in polypropylene pots (height: 7.5 cm and diameter: 8 cm) with a 90 µm mesh at the bottom and a 5 cm high plastic fence (from the top of the pot), to minimize the escape of invertebrates from the pots while allowing for vegetation growth. The pots containing intact soil cores (hereafter referred as microcosms) were transported to the laboratory on the same day of field sampling, weighed, and allocated to lit incubators set at their respective temperature regimes (details in the next section; Table S3). The gravimetric soil water content at the time of sampling was determined by drying five additional soil samples at 70 °C for 48h (Table S2; Fig. S3). We maintained the same water content as in the time of sampling during the entire duration of the experiment (except in the extreme heat treatment during the week of the heat event; details in the following section), by weighing each microcosm every third day and adjusting evaporative losses with deionized water. In order to avoid keeping exceedingly dry soil conditions during the experiments, we made sure that the sampling of soil cores took place shortly after the occurrence of precipitation events in the field sites (> 5 mm during the previous week). Additionally, we took three soil cores across seasons to determine soil pH (Table S2), and one soil core to monitor soil temperature in the incubators over the course of the experiments (collected at a random location within the plots).

Temperature treatments

Ambient (control) temperatures in the incubators were set to simulate the average climatic conditions in the field sites, and were therefore adjusted to the corresponding elevation and season of the samples. We retrieved climatic data of the reference period 2015-2020 from two representative weather

stations (one for each elevation, Table S3). This time reference was chosen due to the increasing frequency of heat waves in the region, especially in recent years (70). Ambient conditions were defined as the mean average daily temperatures of the two months that our microcosms were incubated in the laboratory. For example, samples collected in spring were exposed to the average temperature conditions of May and June as the ambient temperature in our lab experiment for the entire experimental duration of this season. To simulate heat events that were statistically extreme in all elevations and seasons (2, 70), we calculated the 99th percentile of average daily temperature across the reference period (14), and applied this temperature during seven consecutive days (Fig. 1). All ambient and extreme heat temperature values for each season and site are provided in Table S3. We additionally assessed how our experimental extreme heat events compared to naturally occurring heat extremes in the field sites during the study period (details in Table S8).

To imitate typically dry conditions encountered during extreme heat events, microcosms allocated to the extreme heat treatment did not receive any water inputs during the week of the heat event, and water losses were compensated only at the start of the recovery phase (soil water content data shown in Fig. S3). All temperature regimes adopted a diel light and temperature cycle (8h night/ 16h day), with a 6 °C-amplitude between night and day (Table S3). Air temperature and humidity, light intensity and soil temperature (depth 3-5 cm; Fig. 1) were monitored in the incubators (SANYO MIR-253, Japan) at 30-min intervals (HOBO® MX Multi-Channel, Onset Computer Corporation, USA). The incubators (N = 6) were randomly rotated among treatments at each season (Table S3).

Data collection

After field sampling, all soil microcosms were acclimated for one week in the incubators at ambient temperatures. We collected data of soil-living communities of microarthropods (Collembola) and fungi across three harvests for each season. Each microcosm was accordingly allocated to one of three harvests: harvest 1 (week 2 after field sampling, before the extreme heat event), harvest 2 (week 3, immediately after the extreme heat event), and harvest 3 (week 8, after a five-week recovery period

following the extreme heat event). At each harvest, we collected a scoop of moist soil from the bottom of each microcosm to minimize sample disturbance, rather than using the common practice of homogenizing the sample (mean weight subsamples (g) ± SD: 8.55 ± 0.44). The subsamples were then stored at -20 °C until extraction of fungal DNA (March-May 2023). Next, we extracted all microarthropods from the microcosms with gradual heating from 25 °C up to 55 °C for 7 days following the Macfayden extraction method (71). All animals were collected in glycol water solution (1:1) and later transferred to 70% ethanol.

Collembolans were sorted and identified to species level (details in Table S4). We retrieved information on the vertical stratification of Collembola species to examine how this trait mediates species responses to extreme heat. We assigned each species to one of three categories depending on their adaptations to occupy different depths of the soil profile: epedaphic (surface-living), hemiedaphic (living in litter and upper soil layers) and euedaphic (permanently living in the soil). The abundances and vertical stratification of all Collembola species are listed in Table S4.

Fungal ITS metabarcoding

Fungal DNA was extracted from 250 mg of bulk fresh soil (subsamples) using the Qiagen DNAeasy PowerSoil Pro Kit, following the manufacturer's instructions. We then carried out PCR-amplification targeting the primers 'TCCGTAGGTGAACCTGC' (forward) and 'GCATATCAATAAGCGGAGGA' (reverse), followed by amplicon sequencing of the full ITS region (ITS1-ITS2) with PacBio Sequel II instrument (Pacific Biosciences, USA). Libraries were loaded into three SMRTcells, each including five blanks and five controls (listed in Table S5). PCR and amplicon sequencing were conducted at the Next Generation Sequencing Platform of the University of Bern. Processing of the HiFi reads was performed with the pb-16S-nf pipeline (https://github.com/PacificBiosciences/HiFi-16S-workflow), which makes use of QIIME2 (72) and DADA2 (73). Briefly, after demultiplexing, low-quality reads (<Q20) were discarded, primers trimmed (mean read length after processing: 670 bp), and denoised ASVs were obtained. Next, singletons and ASVs with less than five reads were filtered out, and taxonomical assignment with VSEARCH was performed using the UNITE QIIME release 9 (74). We then merged the data from the

different sequencing runs and retained only fungal ASVs agglomerated at the species level (R package phyloseq v. 1.48.0) (75). We also obtained the main trophic strategy of each fungal species (i.e., saprotroph, symbiotroph, pathogenic) using the package FUNGuildR v. 0.2.0.9000 (76). We selected the first annotated trophic strategy for those taxa with mixed trophic modes, and we only retained the trophic strategies assigned with “probable” and “highly probable” confidence (following (76)), treating the remaining as “unassigned”.

Data analyses: total abundances and diversity indices

All analyses were performed in R version 4.4.0 (77). We tested how the effects of extreme heat on belowground communities were modulated by elevation and season, using the following three-way interaction model:

Eq. 1. $Response\ variable \sim Elevation\ x\ Season\ x\ Temperature\ treatment + (1 \mid Site)$

Where *Site* (*N* = 4) was treated as a random factor in all models to control for non-independence among experimental units at each site (69). All models were fitted separately for each experimental harvest: harvest 1 or baseline (H1), harvest 2 or resistance response (H2), and harvest 3 or recovery response (H3; Fig. 1). Linear models with univariate response variables were fitted with the R package glmmTMB v.1.1.9 (78). Linearity assumptions (i.e., normality of residuals, overdispersion, zero-inflation, homogeneity of variance) were verified with the package DHARMa v.0.4.6 (79). We obtained marginal means and contrasts between control and extreme heat treatments using the emmeans package v.1.10.1 (80), and calculated conditional and marginal R^2 of the linear models (81) with the r.squaredGLMM function from the package MuMIn v.1.47.5 (82).

Total Collembola abundances were analyzed with generalized linear mixed-effects models (GLMM) with negative binomial distribution (Eq. 1). We also employed negative binomial GLMMs to analyze the total number of reads for different groups of fungi according to their trophic strategy (saprotrophs, pathogens, symbionts and unassigned fungi), including the log-transformed number of

reads as a covariate to control for variation in sequencing depth across samples (83, 84). The diversity of Collembola and fungi was assessed by means of diversity profiles, obtained across three values of Hill numbers (order *q*): *q* = 0 (species richness), *q* = 1 (Shannon-Hill) and *q* = 2 (Simpson-Hill). The diversity profiles describe how the different diversity metrics change along a gradient of leverage of species' rarity, with lower values of *q* emphasizing the contribution of rare species, while higher values of *q* heighten the contribution of more common species (85). We computed diversity estimates using coverage-based rarefaction and extrapolation to equalize samples (coverage value of 0.90 for Collembola, and 0.98 for fungi) with the iNEXT package v.3.0.1 (86, 87). The resulting point estimates of diversity were tested using linear mixed models (Eq. 1) with Gaussian distribution. Before calculating the diversity indices, we applied an abundance cut-off to restrict the diversity analysis to samples with at least ten individuals (only needed for Collembola).

Data analyses: species abundances and association networks

Species abundances were evaluated using joint species distribution models (jSDMs) (88, 89) within the Hierarchical Modelling of Species Communities framework (package Hmsc v.3.0-13) (90), assuming default prior distributions (91). The ecological interpretation of the parameters estimated with the jSDMs is shown in Table S6. Block (*N* = 2) was added as a random effect in all fitted jSDMs to account for variation in species occurrences driven by their large-scale geographic distributions (see Fig. S5). We adopted a prevalence threshold of 25% to discard rare taxa (i.e., species occurring in less than 30 out of the 120 experimental units sampled at each harvest), which may provide low statistical power due to the scarcity of data (e.g., (92)). In the jSDMs, we performed variance partitioning to extract the proportion of total variance explained by the experimental treatment (extreme heat), the natural variables (elevation and season), and the random effects (site and block). We built three sets of models with different groups of response variables: 1) the Collembola model, measuring responses of Collembola communities; 2) the fungi model, assessing responses of fungal communities; and 3) the Collembola-fungi models, examining associations between Collembola and fungi (details below). First, in the

Collembola model, we used the log-normal Poisson distribution (analogous to negative binomial distribution) (91). We further modelled the influence of the species' traits on their abundance responses, by including the species' vertical stratification as a factor variable with three levels (epedaphic, hemiedaphic, and euedaphic). Second, in the fungal model, we accounted for zero-inflation, as typically encountered in sequencing data, by constructing a hurdle model that consisted of two parts: presence-absence (modelled with probit regression), and abundance conditional on presence (linear regression with normal distribution, using log-transformed and scaled counts). We further controlled for variation in sequencing depth by including the log-transformed number of reads as a covariate (83, 84). We additionally included the fungal species' trophic strategy in the models as a factor variable with four levels (saprotrophs, symbionts, pathogens, and unassigned), to examine how this trait can mediate fungal occurrence and abundance responses. The explanatory power of the jSDMs was evaluated by means of pseudo-R^2 (Collembola model), Tjur R^2 (presence-absence part of the fungal model) and R^2 (abundance part of the fungal model) (91). MCMC convergence for all estimated parameters was assessed in terms of potential scale reduction factors (Table S7) (93). All jSDMs were fitted with four chains of 250 samples each, yielding 1000 posterior samples in total. The thinning intervals and the number of samples used as burn-in were adjusted for the different models according to the amount required to achieve adequate model convergence (Table S7) (Collembola model: thinning 1,000 and burn-in 125,000; fungal models: thinning 300 and burn-in 37,500; Collembola-fungi association models: thinning 100 and burn-in 12,500).

The third set of jSDMs (Collembola-fungi models) allowed us to estimate associations between Collembola and fungi, followed by the analysis of network properties to summarize these associations at the network level. We focused this analysis on the recovery response to gain more robust and ecologically meaningful insights into the role of biotic effects in mediating responses to extreme heat. Resistance responses are primarily driven by abiotic effects of extreme heat on species' abundances, while recovery responses can be more strongly influenced by biotic effects, such as associations with other species (7). This is because heat-driven changes in the abundance of one species (e.g., fungi) may take time to affect the abundance of a second species (e.g., Collembola). We assume that our measurement of recovery (i.e., five weeks after the end of the extreme heat events) can generally capture

such a time lag in disturbance effects across the two trophic levels (94). For this analysis, we created separate subsets from the full dataset for each elevation and season, resulting in six subsets, each containing 20 samples. We applied a prevalence threshold of 25% within each subset (i.e., discarding species occurring in fewer than five samples) for all Collembola and fungal species, as previously described. Due to the very low prevalence of Collembola species in summer at low elevation, we could not determine associations in this case. Next, we built the jSDMs using fungal species abundances as response variables (log-transformed and scaled abundances, conditional on presence), while treating Collembola species abundances (log-transformed +1 and scaled) and their interactive effects with extreme heat as explanatory variables. We retained the associations between Collembola and fungi with 95% credible intervals not overlapping zero for control and extreme heat treatments, using the ci function from the bayestestR package v. 0.15.0 (95). Extreme heat associations were obtained by summing the parameter estimates of every Collembola-fungal association in the control treatment and the interactive effects of extreme heat, in all posterior samples. These associations can be indicative of bottom-up regulation through feeding (positive associations) or repulsion (negative associations), but they should be interpreted with care, as they may also capture the signal of joint responses to unmeasured abiotic variables (89, 96). Additionally, the mismatch in the spatial scales at which Collembola and fungi were measured (see Data collection in Methods) may lessen the statistical signal of their associations (96), particularly due to small-scale variation in fungal composition within the soil cores (97) (although experimental replication partly accounts for this issue; see Fig. S5).

After fitting the jSDMs, we examined how two association network properties differed between control and extreme heat treatments: connectance and network dissimilarity. We visualized the associations resulting from the Collembola-fungi jSDMs using the igraph package v.2.0.2 (98). For the analysis of connectance (i.e., the ratio of the number of realized associations to the number of potential associations) (99), we calculated the observed differences in network connectance between the experimental treatments, and further generated null models to test how the observed differences diverged from random expectations. To do this, we first trimmed the control and extreme heat networks obtained from the same jSDM (i.e., same spatiotemporal context) to retain only the species having associations in

either of the two networks (metaweb). We then produced 1000 permutations of each association network using the r2dtable algorithm (implemented in the package vegan v.2.6-4) (100), as this method keeps the matrix dimensions and marginal totals constant while allowing for variation in the number of non-zero elements (i.e., number of Collembola-fungal associations), and hence connectance (101). We then calculated differences in connectance between the random networks from control and extreme heat treatments, and compared these to the observed differences. To do so, we computed z-scores (Eq. 2), and obtained the corresponding p-values using two-tailed tests of population proportion.

$$\text{Eq. 2} \quad z = \frac{Observed\ connectance\ difference - Mean\ null\ connectance\ differences}{SD\ null\ connectance\ differences}$$

To pinpoint the specific fungal groups driving changes in network connectance, we repeated the connectance analysis separately for saprotrophic and pathogenic fungi. Finally, we assessed the dissimilarity of control and extreme heat networks (using presence-absence of associations, as in the connectance analysis), and partitioned network differences into their compositional (i.e., differences in the composition of the species between the networks) and rewiring components (i.e., dissimilarity in the associations among shared species in control and extreme heat networks) (102), with the betalinkr function implemented in the bipartite package v.2.20 (103).

Data and code availability statement

The complete dataset and R scripts used in this study are available in the Figshare repository: https://figshare.com/s/6e97dcd9e93c64ff6b60.

Acknowledgments

We thank the managers of the field sites for their collaboration throughout the study: Hôtel Chasseral, Pro Natura Neuchâtel, communes of Onnens and Bullet, and canton Vaud. We greatly appreciate the assistance of Laurent Dubied, Anine Wyser, Elisenda Peris i Morente, Arianne Marty, Gaia Giacomelli, Silvan Zünd and Shareen Sanders during the field sampling and lab work. We are grateful to the Next Generation Sequencing Platform of the University of Bern, particularly Simone Oberhänsli and Pamela Nicholson, for performing the sequencing experiments and providing support for the bioinformatic analyses. The manuscript benefited from valuable discussions with Nerea Abrego, Jordi Bascompte, Jaume A. Badia-Boher, and members of the Terrestrial Ecology group at the University of Bern. This work was supported by the Swiss State Secretariat for Education, Research and Innovation (SERI) under contract number M822.00029 and from the Swiss National Science Foundation (grant number: 310030_212550).

References

1. R. M. B. Harris, *et al.*, Biological responses to the press and pulse of climate trends and extreme events. *Nat. Clim. Change* **8**, 579–587 (2018).

2. IPCC, “Summary for Policymakers” (2023).

3. M. P. Thakur, A. C. Risch, W. H. Van der Putten, Biotic responses to climate extremes in terrestrial ecosystems. *iScience* **25**, 104559 (2022).

4. C.-S. Ma, G. Ma, S. Pincebourde, Survive a Warming Climate: Insect Responses to Extreme High Temperatures. *Annu. Rev. Entomol.* **66**, 8.1-8.22 (2020).

5. C. M. Williams, *et al.*, Biological impacts of thermal extremes: mechanisms and costs of functional responses matter. *Integr. Comp. Biol.* **56**, 73–84 (2016).

6. L. B. Buckley, J. G. Kingsolver, Evolution of Thermal Sensitivity in Changing and Variable Climates. *Annu. Rev. Ecol. Evol. Syst.* **52**, 563–586 (2021).

7. G. Martínez-De León, M. P. Thakur, Ecological debts induced by heat extremes. *Trends Ecol. Evol.* **39**, 1024–1034 (2024).

8. S. E. Williams, L. P. Shoo, J. L. Isaac, A. A. Hoffmann, G. Langham, Towards an integrated framework for assessing the vulnerability of species to climate change. *PLoS Biol.* **6**, e325 (2008).

9. J. M. Sunday, *et al.*, Thermal tolerance patterns across latitude and elevation. *Philos. Trans. R. Soc. B Biol. Sci.* **374**, 20190036 (2019).

10. C. A. Deutsch, *et al.*, Impacts of climate warming on terrestrial ectotherms across latitude. *Proc. Natl. Acad. Sci. U. S. A.* **105**, 6668–6672 (2008).

11. J. G. Kingsolver, S. E. Diamond, L. B. Buckley, Heat stress and the fitness consequences of climate change for terrestrial ectotherms. *Funct. Ecol.* **27**, 1415–1423 (2013).

12. A. M. Louthan, M. L. DeMarche, L. G. Shoemaker, Climate sensitivity across latitude: scaling physiology to communities. *Trends Ecol. Evol.* **36**, 931–942 (2021).

13. E. Cinto Mejía, W. C. Wetzel, The ecological consequences of the timing of extreme climate events. *Ecol. Evol.* **13**, e9661 (2023).

14. A. Jentsch, J. Kreyling, C. Beierkuhnlein, A new generation of climate-change experiments: events, not trends. *Front. Ecol. Environ.* **5**, 365–374 (2007).

15. C.-S. Ma, L. Wang, W. Zhang, V. H. W. Rudolf, Resolving biological impacts of multiple heat waves: interaction of hot and recovery days. *Oikos* **127**, 622–633 (2018).

16. B. S. Walsh, *et al.*, The Impact of Climate Change on Fertility. *Trends Ecol. Evol.* **34**, 249–259 (2019).

17. J. Forrest, A. J. Miller-Rushing, Toward a synthetic understanding of the role of phenology in ecology and evolution. *Philos. Trans. R. Soc. B Biol. Sci.* **365**, 3101–3112 (2010).

18. G. Martínez-De León, A. Marty, M. Holmstrup, M. P. Thakur, Population resistance and recovery after an extreme heat event are explained by thermal effects on life-history traits. *Oikos* **2024**, e10023 (2024).

19. K. E. Coblentz, *et al.*, A framework for understanding climate change impacts through non-compensatory intra- and interspecific climate change responses. *Glob. Change Biol.* **30**, e17378 (2024).

20. N. Pilakouta, L. Sellers, R. Barratt, A. Ligonniere, The consequences of heatwaves for animal reproduction are timing-dependent. *Funct. Ecol.* **37**, 2425–2433 (2023).

21. T. Roslin, *et al.*, Phenological shifts of abiotic events, producers and consumers across a continent. *Nat. Clim. Change* **11**, 241–248 (2021).

22. M. K. Sundqvist, N. J. Sanders, D. A. Wardle, Community and ecosystem responses to elevational gradients: Processes, mechanisms, and insights for global change. *Annu. Rev. Ecol. Evol. Syst.* **44**, 261–280 (2013).

23. C. Körner, The use of “altitude” in ecological research. *Trends Ecol. Evol.* **22**, 569–574 (2007).

24. I. D. Hodkinson, Terrestrial insects along elevation gradients: Species and community responses to altitude. *Biol. Rev. Camb. Philos. Soc.* **80**, 489–513 (2005).

25. L. B. Buckley, S. D. Schoville, C. M. Williams, Shifts in the relative fitness contributions of fecundity and survival in variable and changing environments. *J. Exp. Biol.* **224**, 1–9 (2021).

26. B. J. Kefford, *et al.*, Acute, diel, and annual temperature variability and the thermal biology of ectotherms. *Glob. Change Biol.* **28**, 6872–6888 (2022).

27. C. M. Sgrò, J. S. Terblanche, A. A. Hoffmann, What Can Plasticity Contribute to Insect Responses to Climate Change? *Annu. Rev. Entomol.* **61**, 433–451 (2016).

28. B. van Heerwaarden, C. M. Sgrò, Male fertility thermal limits predict vulnerability to climate warming. *Nat. Commun.* **12**, 2214 (2021).

29. M. P. Berg, *et al.*, Adapt or disperse: Understanding species persistence in a changing world. *Glob. Change Biol.* **16**, 587–598 (2010).

30. O. Franken, M. Huizinga, J. Ellers, M. P. Berg, Heated communities: large inter- and intraspecific variation in heat tolerance across trophic levels of a soil arthropod community. *Oecologia* **186**, 311–322 (2018).

31. M. P. Thakur, Climate warming and trophic mismatches in terrestrial ecosystems: The Green–Brown imbalance hypothesis. *Biol. Lett.* **16**, 20–22 (2020).

32. S. J. Thackeray, *et al.*, Trophic level asynchrony in rates of phenological change for marine, freshwater and terrestrial environments. *Glob. Change Biol.* **16**, 3304–3313 (2010).

33. M. Delgado-Baquerizo, *et al.*, Multiple elements of soil biodiversity drive ecosystem functions across biomes. *Nat. Ecol. Evol.* **4**, 210–220 (2020).

34. M. M. Pollierer, S. Scheu, Stable isotopes of amino acids indicate that soil decomposer microarthropods predominantly feed on saprotrophic fungi. *Ecosphere* **12**, e03425 (2021).

35. A. A. Potapov, E. E. Semenina, A. Yu, N. A. Kuznetsova, A. V. Tiunov, Connecting taxonomy and ecology: Trophic niches of collembolans as related to taxonomic identity and life forms. *Soil Biol. Biochem.* **101**, 20–31 (2016).

36. J. C. Moore, H. W. Hunt, Resource compartmentation and the stability of real ecosystems. *Nature* **333**, 261–263 (1988).

37. M. P. Thakur, S. Geisen, Trophic Regulations of the Soil Microbiome. *Trends Microbiol.* **27**, 771–780 (2019).

38. C. G. Knight, *et al.*, Soil microbiomes show consistent and predictable responses to extreme events. *Nature* (2024). https://doi.org/10.1038/s41586-024-08185-3.

39. F. T. de Vries, *et al.*, Soil bacterial networks are less stable under drought than fungal networks. *Nat. Commun.* **9** (2018).

40. F. T. de Vries, *et al.*, Land use alters the resistance and resilience of soil food webs to drought. *Nat. Clim. Change* **2**, 276–280 (2012).

41. R. D. Bardgett, T. Caruso, Soil microbial community responses to climate extremes: Resistance, resilience and transitions to alternative states. *Philos. Trans. R. Soc. B Biol. Sci.* **375** (2020).

42. I. Cordero, A. Leizeaga, L. C. Hicks, J. Rousk, R. D. Bardgett, High intensity perturbations induce an abrupt shift in soil microbial state. *ISME J.* **17**, 2190–2199 (2023).

43. S. K. D. Sanders, G. Martínez-De León, L. Formenti, M. P. Thakur, How will climate change affect the feeding biology of Collembola ? *Soil Biol. Biochem.* **188**, 109244 (2024).

44. M. Delgado-Baquerizo, *et al.*, The proportion of soil-borne pathogens increases with warming at the global scale. *Nat. Clim. Change* **10**, 550–554 (2020).

45. N. Blüthgen, J. Fründ, D. P. Vazquez, F. Menzel, What do interaction network metrics tell us about specialization and biological traits? *Ecology* **89**, 3387–3399 (2008).

46. O. L. Petchey, U. Brose, B. C. Rall, Predicting the effects of temperature on food web connectance. *Philos. Trans. R. Soc. B Biol. Sci.* **365**, 2081–2091 (2010).

47. M. E. Dillon, G. Wang, R. B. Huey, Global metabolic impacts of recent climate warming. *Nature* **467**, 704–706 (2010).

48. M. P. Thakur, B. D. Sigurðsson, P. Sigurðsson, M. Holmstrup, Warming shifts the biomass distribution of soil microarthropod communities. *Soil Biol. Biochem.* **177**, 108894 (2023).

49. C. van Dooremalen, M. P. Berg, J. Ellers, Acclimation responses to temperature vary with vertical stratification: Implications for vulnerability of soil-dwelling species to extreme temperature events. *Glob. Change Biol.* **19**, 975–984 (2013).

50. J. M. Sunday, *et al.*, Thermal-safety margins and the necessity of thermoregulatory behavior across latitude and elevation. *Proc. Natl. Acad. Sci. U. S. A.* **111**, 5610–5615 (2014).

51. N. Tüzün, R. Stoks, Evolution of geographic variation in thermal performance curves in the face of climate change and implications for biotic interactions. *Curr. Opin. Insect Sci.* **29**, 78–84 (2018).

52. K. M. Baudier, C. L. D'Amelio, R. Malhotra, M. P. O'Connor, S. O'Donnell, Extreme insolation: Climatic variation shapes the evolution of thermal tolerance at multiple scales. *Am. Nat.* **192**, 347–359 (2018).

53. L. B. Buckley, E. F. Miller, J. G. Kingsolver, Ectotherm thermal stress and specialization across altitude and latitude. *Integr. Comp. Biol.* **53**, 571–581 (2013).

54. N. A. Moore, *et al.*, Temperate species underfill their tropical thermal potentials on land. *Nat. Ecol. Evol.* **7**, 1993–2003 (2023).

55. M. Holmstrup, M. Bayley, *Protaphorura tricampata*, a euedaphic and highly permeable springtail that can sustain activity by osmoregulation during extreme drought. *J. Insect Physiol.* **59**, 1104–1110 (2013).

56. Q. Bei, *et al.*, Extreme summers impact cropland and grassland soil microbiomes. *ISME J.* **17**, 1589–1600 (2023).

57. A. Guhr, W. Borken, M. Spohn, E. Matzner, Redistribution of soil water by a saprotrophic fungus enhances carbon mineralization. *Proc. Natl. Acad. Sci. U. S. A.* **112**, 14647–14651 (2015).

58. G. J. Pec, *et al.*, Fungal community response to long-term soil warming with potential implications for soil carbon dynamics. *Ecosphere* **12** (2021).

59. Y. Feng, *et al.*, Temperature thresholds drive the global distribution of soil fungal decomposers. *Glob. Change Biol.* **28**, 2779–2789 (2022).

60. S. Masaki, Summer Diapause. *Annu. Rev. Entomol.* **25**, 1–25 (1980).

61. J. G. Testerink, Metabolic adaptations to seasonal changes in humidity and temperature in litter-inhabiting Collembola. *Oikos* **40**, 234–240 (1983).

62. S. Anslan, M. Bahram, L. Tedersoo, Seasonal and annual variation in fungal communities associated with epigeic springtails (Collembola spp.) in boreal forests. *Soil Biol. Biochem.* **116**, 245–252 (2018).

63. K. M. Dromph, S. Vestergaard, Pathogenicity and attractiveness of entomopathogenic hyphomycete fungi to collembolans. *Appl. Soil Ecol.* **21**, 197–210 (2002).

64. M. E. Nielsen, P. Lehmann, K. Gotthard, Longer and warmer prewinter periods reduce post-winter fitness in a diapausing insect. *Funct. Ecol.* **36**, 1151–1162 (2022).

65. O. L. Cope, L. N. Zehr, A. A. Agrawal, W. C. Wetzel, The timing of heat waves has multiyear effects on milkweed and its insect community. *Ecology* **104**, e3988 (2023).

66. A. I. Dell, S. Pawar, V. M. Savage, Systematic variation in the temperature dependence of physiological and ecological traits. *Proc. Natl. Acad. Sci. U. S. A.* **108**, 10591–10596 (2011).

67. F. Polazzo, M. Hermann, M. Crettaz-Minaglia, A. Rico, Impacts of extreme climatic events on trophic network complexity and multidimensional stability. *Ecology* **104**, e3951 (2023).

68. G. P. Quinn, M. J. Keough, *Experimental Design and Data Analysis for Biologists* (Cambridge University Press, 2002).

69. H. Schielzeth, S. Nakagawa, Nested by design: Model fitting and interpretation in a mixed model era. *Methods Ecol. Evol.* **4**, 14–24 (2013).

70. CH2018, *CH2018 – Climate Scenarios for Switzerland, Technical Report* (National Centre for Climate Services, 2018).

71. A. Macfadyen, Improved Funnel-Type Extractors for Soil Arthropods. *J. Anim. Ecol.* **30**, 171–184 (1961).

72. E. Bolyen, *et al.*, Reproducible, interactive, scalable and extensible microbiome data science using QIIME 2. *Nat. Biotechnol.* **37**, 852–857 (2019).

73. B. J. Callahan, *et al.*, DADA2: High-resolution sample inference from Illumina amplicon data. *Nat. Methods* **13**, 581–583 (2016).

74. K. Abarenkov, *et al.*, UNITE QIIME release for eukaryotes 2. *UNITE Community* (2023).

75. P. J. McMurdie, S. Holmes, Phyloseq: An R Package for Reproducible Interactive Analysis and Graphics of Microbiome Census Data. *PLoS ONE* **8** (2013).

76. N. H. Nguyen, *et al.*, FUNGuild: An open annotation tool for parsing fungal community datasets by ecological guild. *Fungal Ecol.* **20**, 241–248 (2016).

77. R Core Team, R: A language and environment for statistical computing. (2024). https://doi.org/10.1108/eb003648. Deposited 2024.

78. M. E. Brooks, *et al.*, glmmTMB balances speed and flexibility among packages for zero-inflated generalized linear mixed modeling. *R J.* **9**, 378–400 (2017).

79. F. Hartig, DHARMa: Residual Diagnostics for Hierarchical (Multi-Level / Mixed) Regression Models. (2022). Deposited 2022.

80. R. V. Lenth, emmeans: Estimated Marginal Means, aka Least-Squares Means. (2024). Deposited 2024.

81. S. Nakagawa, H. Schielzeth, A general and simple method for obtaining R2 from generalized linear mixed-effects models. *Methods Ecol. Evol.* **4**, 133–142 (2013).

82. K. Bartón, MuMIn: Multi-Model Inference. R package version 1.47.5. (2023). Deposited 2023.

83. M. F. A. Leite, E. E. Kuramae, You must choose, but choose wisely: Model-based approaches for microbial community analysis. *Soil Biol. Biochem.* **151**, 108042 (2020).

84. L. Tedersoo, *et al.*, Best practices in metabarcoding of fungi: From experimental design to results. *Mol. Ecol.* **31**, 2769–2795 (2022).

85. M. Roswell, J. Dushoff, R. Winfree, A conceptual guide to measuring species diversity. *Oikos* **130**, 321–338 (2021).

86. A. Chao, *et al.*, Rarefaction and extrapolation with Hill numbers: A framework for sampling and estimation in species diversity studies. *Ecol. Monogr.* **84**, 45–67 (2014).

87. T. C. Hsieh, K. H. Ma, A. Chao, iNEXT: iNterpolation and EXTrapolation for species diversity. (2022). Deposited 2022.

88. D. I. Warton, *et al.*, So Many Variables : Joint Modeling in Community Ecology. **30**, 766–779 (2015).

89. O. Ovaskainen, *et al.*, How to make more out of community data? A conceptual framework and its implementation as models and software. *Ecol. Lett.* **20**, 561–576 (2017).

90. G. Tikhonov, *et al.*, Hmsc: Hierarchical Model of Species Communities. (2022). Deposited 2022.

91. O. Ovaskainen, N. Abrego, *Joint Species Distribution Modelling: With Applications in R* (Cambridge University Press, 2020).

92. S. Burg, *et al.*, Experimental evidence that root-associated fungi improve plant growth at high altitude. *Mol. Ecol.* **33**, e17376 (2024).

93. A. Gelman, D. B. Rubin, Inference from Iterative Simulation Using Multiple Sequences. *Stat. Sci.* **7**, 457–472 (1992).

94. M. C. Jackson, S. Pawar, G. Woodward, The Temporal Dynamics of Multiple Stressor Effects: From Individuals to Ecosystems. *Trends Ecol. Evol.* **36**, 402–410 (2021).

95. D. Makowski, M. Ben-Shachar, D. Lüdecke, bayestestR: Describing Effects and their Uncertainty, Existence and Significance within the Bayesian Framework. *J. Open Source Softw.* **4**, 1541 (2019).

96. F. G. Blanchet, K. Cazelles, D. Gravel, Co-occurrence is not evidence of ecological interactions. *Ecol. Lett.* **23**, 1050–1063 (2020).

97. A. Erktan, D. Or, S. Scheu, The physical structure of soil: Determinant and consequence of trophic interactions. *Soil Biol. Biochem.* **148**, 107876 (2020).

98. G. Csárdi, *et al.*, igraph: Network Analysis and Visualization in R. (2024). https://doi.org/10.5281/zenodo.7682609. Deposited 2024.

99. R. M. May, Will a Large Complex System be Stable? *Nature* **238**, 413–414 (1972).

100. J. Oksanen, *et al.*, vegan: Community Ecology Package. (2022). Deposited 2022.

101. C. F. Dormann, J. Frund, N. Bluthgen, B. Gruber, Indices, Graphs and Null Models: Analyzing Bipartite Ecological Networks. *Open Ecol. J.* **2**, 7–24 (2009).

102. T. Poisot, E. Canard, D. Mouillot, N. Mouquet, D. Gravel, The dissimilarity of species interaction networks. *Ecol. Lett.* **15**, 1353–1361 (2012).

103. C. F. Dormann, B. Gruber, J. Fründ, Introducing the bipartite Package: Analysing Ecological Networks. **8/2**, 8–11 (2008).

Figures

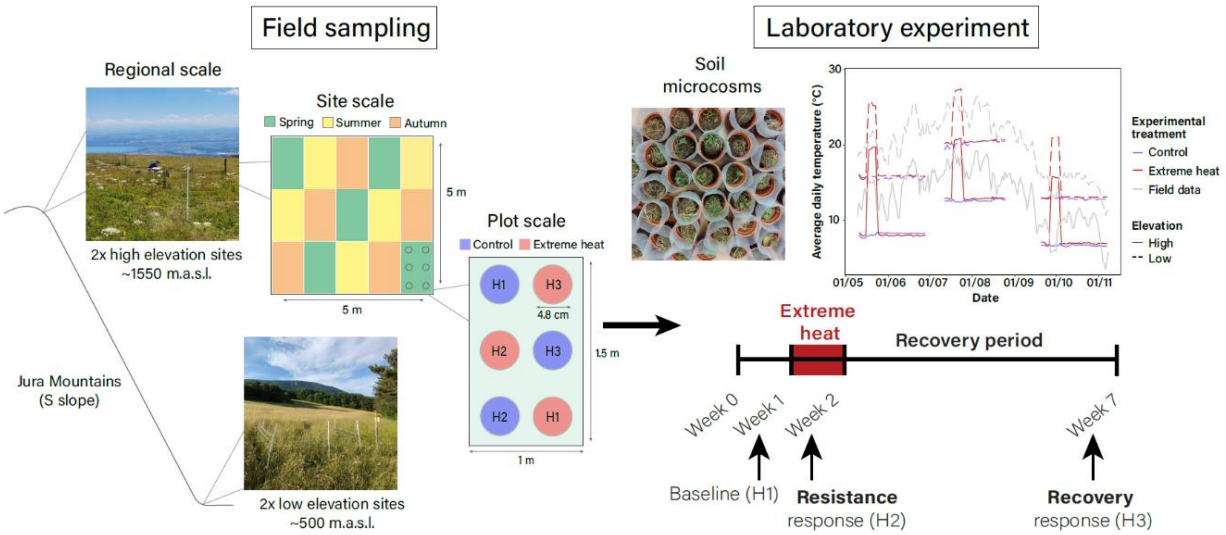

Figure 1. Scheme of the experimental design of the study. We used a split-plot sampling design (left side of the figure), whereby samples (intact soil cores) were taken from two regional-scale blocks, each containing one high- and one low-elevation site (Fig. S1). Sites were defined as a delineated 5 x 5 m area representative of the dry grasslands of the study region (pictures in Fig. S2). Within sites and seasons (i.e., spring, summer, autumn), six soil cores were obtained from each of five 1 m x 1.5 m plots. The sampling locations of data-level predictors (temperature regimes and harvests) were randomized within each plot, whereas the sampling locations of plot-level predictors (seasons) were kept constant in all sites to avoid the sampling from adjacent plots in the same season. The pictures displayed in the figure were taken in the summer season from one of our high (above: Chasseron) and low (below: Onnens) elevation sites (site-specific information is provided in Table S1). The colors of the plots (site scale) denote different sampling seasons: spring (green), summer (yellow) and autumn (orange). The circles shown at the plot scale represent the soil cores used as microcosms in the laboratory experiment (right side of the figure), which were allocated to one of two temperature treatments (control: blue; extreme heat: red) and one of three harvests (H1: baseline or harvest 1; H2: resistance phase or harvest 2; H3: recovery phase or harvest 3). All harvests were destructive, meaning experimental replications were true for each harvest. The size of the soil cores relative to the plot is enhanced for visualization purposes. Average daily soil temperatures (depth 3-5 cm) measured over the course of the laboratory experiments are shown, together with the temperatures recorded in the field sites during the same period (6 May – 9 November 2022). Mean temperatures from the two sites at the same elevation are displayed as grey lines; site-specific temperature values are provided in Fig. S4.

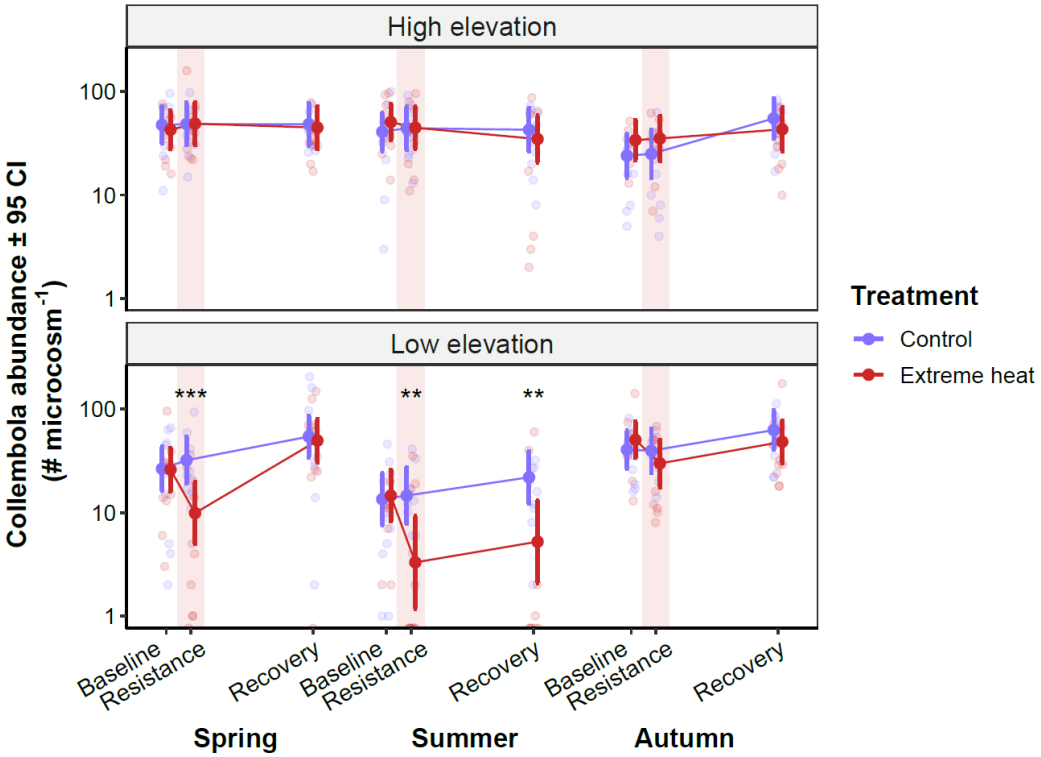

Figure 2. Responses of Collembola abundance to experimental extreme heat events across elevations and at different seasons. Estimated marginal means (± 95 confidence intervals) of Collembola abundance (log-transformed) are shown over the course of the experiments in spring, summer and autumn. The labels on the x-axis specify the different time points in which Collembola densities were assessed during the experiment (i.e., harvests): baseline (harvest 1); resistance phase (harvest 2); recovery phase (harvest 3). The faded red areas represent the one-week extreme heat events. Colours indicate different experimental temperature treatments: blue: control; red: extreme heat. Asterisks show significant differences between treatments at each harvest: $^{**}P < 0.01$, $^{***}P < 0.001$. Full model outputs are provided in Table S9.

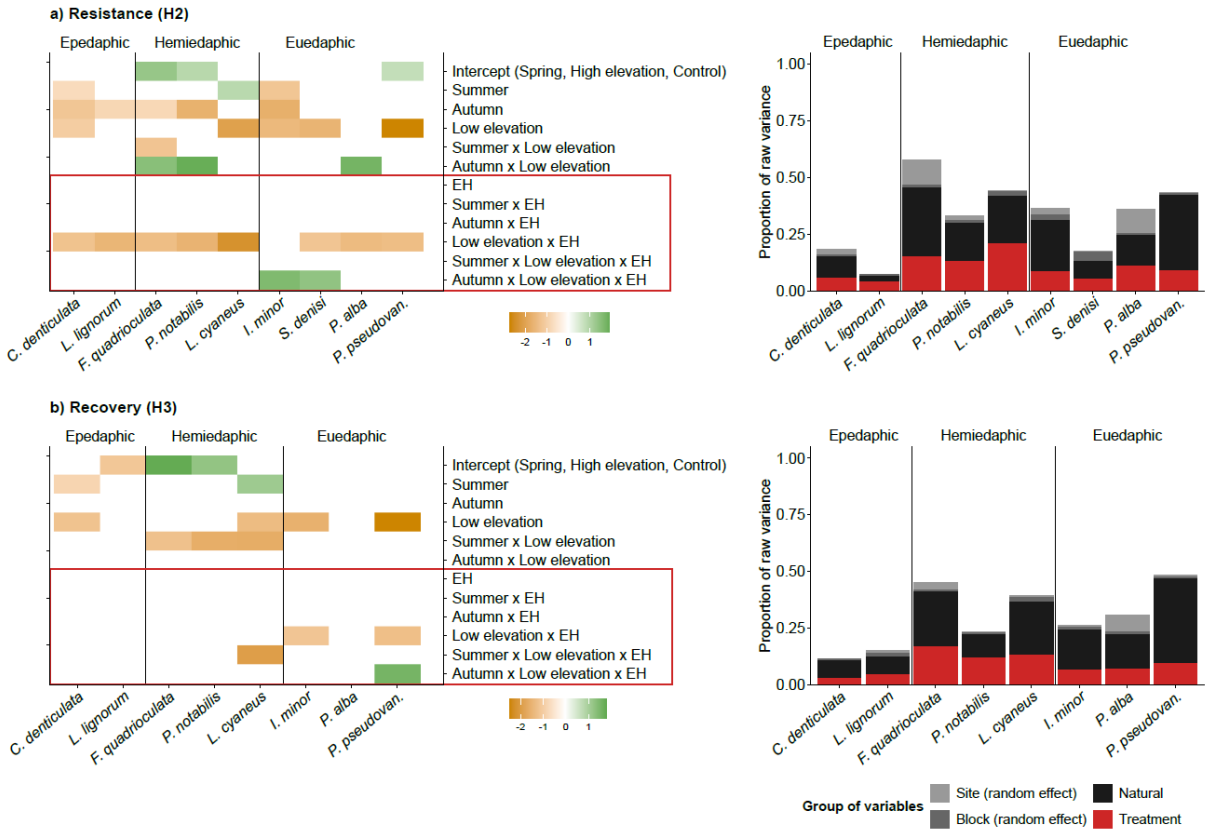

Figure 3. Output of the joint species distribution models (jSDMs) fitted to investigate the responses of Collembola species abundances. We tested the effects of season, elevation, treatment, and their three-way interactions, in the resistance (a; harvest 2: H2; panels above) and the recovery response (b; harvest 3: H3; panels below). The results from the baseline response are provided in Fig. S7. Estimates from the beta parameters (left panels) show the responses of species abundances (x-axis) to each of the model parameters (y-axis). Green and orange colors indicate positive and negative responses with 95% posterior probability, respectively, while blank spaces denote responses that lacked statistical support (should, therefore, be interpreted as neutral response). Species abundances at the intercept (spring, high elevation, control treatment) denote more abundant species in green, less abundant species in orange, and blank spaces indicating intermediate abundances (Table S6). Parameters enclosed within the red area represent species responses to the experimental treatment (extreme heat: EH; see Table S6 for an ecological interpretation of the model parameters). The proportion of raw explained variance (right panels) is provided for different groups of variables: random effects (site and block), natural variables (season and elevation), and treatment (containing the variance explained by all parameters influenced by extreme heat, shown within the red area of the left panels). Collembola species are ordered according to their vertical stratification across the soil profile: epedaphic (surface-living), hemi-edaphic (living in litter and shallow soil layers), and euedaphic (permanently living in the soil).

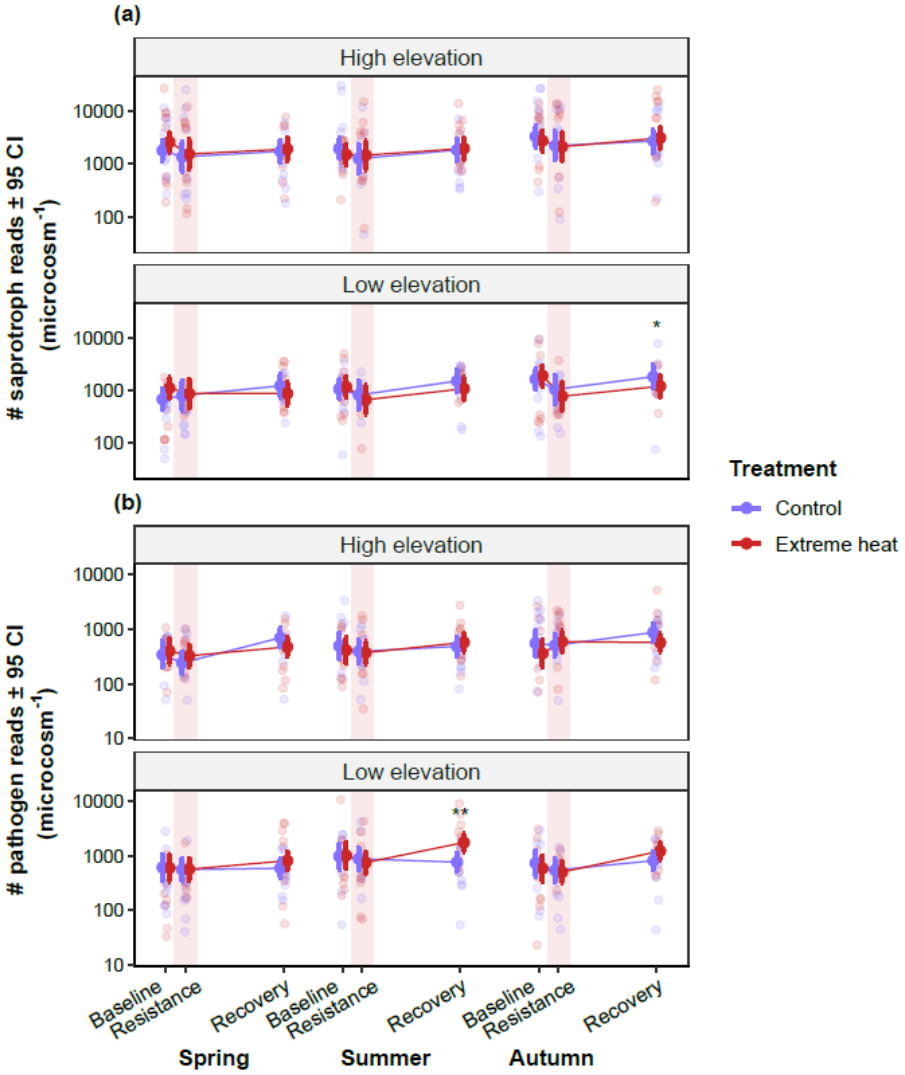

Figure 4. Responses of saprotrophic and pathogenic fungi to experimental extreme heat events across elevations and at different seasons. Estimated marginal means (± 95 confidence intervals) of the number of reads (log-transformed) of saprotrophs (a; upper panel) and pathogenic fungi (b; lower panel) over the course of the experiments in spring, summer and autumn. The labels on the x-axis specify the different time points in which fungal metabarcoding reads were assessed during the experiment (i.e., harvests): baseline (harvest 1); resistance phase (harvest 2); recovery phase (harvest 3). The faded red areas represent the one-week extreme heat events. Colours indicate different experimental temperature treatments: blue: control; red: extreme heat. Stars show significant differences between treatments at each harvest: *$P < 0.05$, **$P < 0.01$. Full model outputs are provided in Tables S10-S11.

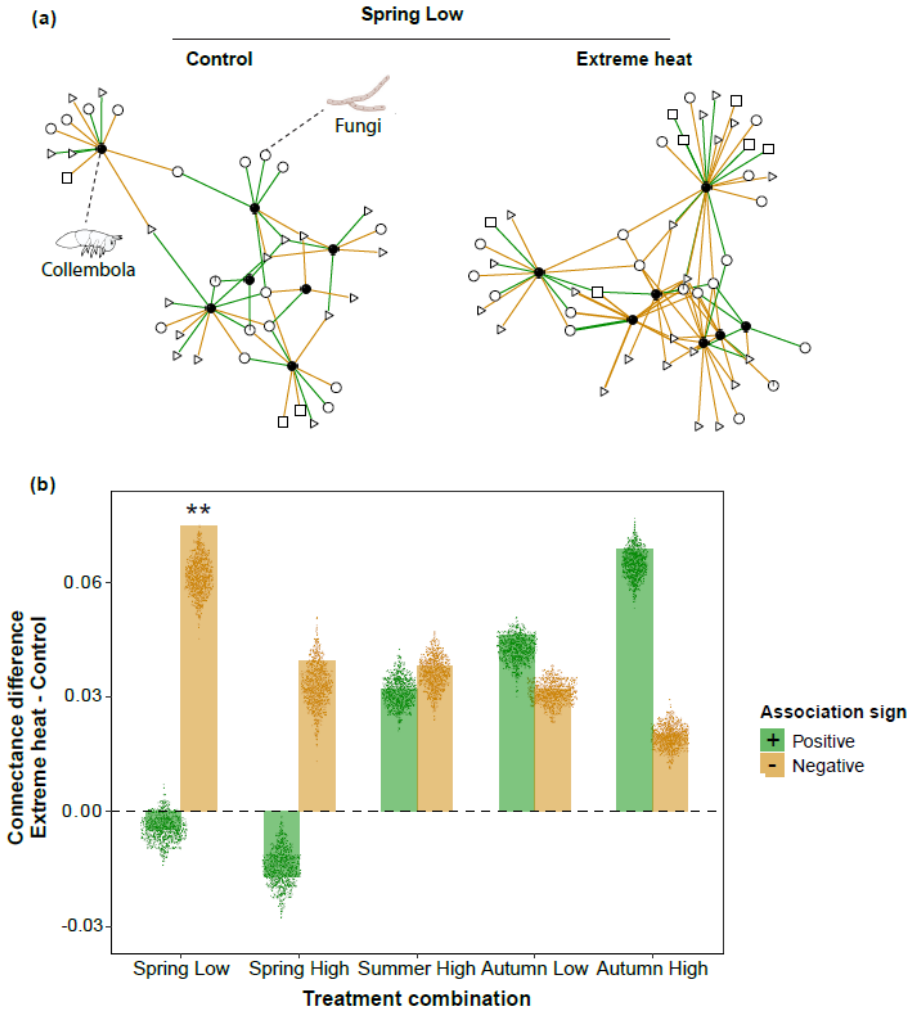

Figure 5. Collembola-fungal association networks and connectance at the recovery response. (a) Comparison of Collembola-fungal association networks between control and extreme heat treatments. An example is shown from the association networks from spring at low elevation. Positive links are displayed with green colors and negative links are shown with orange colors. The width of the links is proportional to the strength of the associations (i.e., parameter estimates of the Collembola-fungal jSDM). Black and white nodes denote Collembola and fungal species, respectively. Different node shapes represent various fungal trophic groups: saprotrophs (circle), pathogens (square), symbionts (pie), and unassigned fungi (triangle). Nodes without associations (i.e., degree = 0) are not displayed. (b) The differences in connectance between extreme heat and control treatments were calculated and tested against those differences obtained from null models. The height of the barplot shows the observed connectance differences, while the points display the connectance differences from the null models. Positive values indicate higher connectance in extreme heat treatments, whereas negative values denote higher connectance in control treatments. Z-scores and p-values are provided in Table S12. Stars show significant greater observed connectance differences between treatments compared to networks generated from the null models: $^{**}P < 0.01$. All association networks are shown in Fig. S15.

Supporting Information for

Belowground communities in lowlands are less stable to climate extremes across seasons

Gerard Martínez-De León[1, *], Ludovico Formenti[1], Jörg-Alfred Salamon[2], Madhav P. Thakur[1]

[1] *Institute of Ecology and Evolution, University of Bern, Switzerland*
[2] *Institute of Animal Ecology & Field Station Schapen, University of Veterinary Medicine Hannover, Germany*

*Corresponding author

Email: gerard.martinezdeleon@unibe.ch

Table of contents

Table S1. Description of the field sites. All plots were located in extensively managed dry meadows (i.e. one hay cut per year occurring not before July 1st and/or low-intensity grazing, no inputs of fertilizer or irrigation), with no recent soil disturbances.

Location	**Chasseral**	**Le Landeron**	**Chasseron**	**Onnens**
Block	North	North	South	South
Elevation	High (1558 m)	Low (481 m)	High (1565 m)	Low (540 m)
Coordinates	47°07'43" N 7°02'52" E	47°03'39" N 7°03'49" E	46°50'58" N 6°32'18? E	46°50'49" N 6°41'07" E
Aspect	170° (S)	210° (SSW)	190° (S)	140° (SE)
Slope	6%	21%	10%	5%
Mowing (frequency, period)	Annually; August-September	Biannually; July-August	No mowing	Annually; July-August
Grazing (type, period)	Not grazed	Not grazed	Cow grazing in the past years, currently not grazed	Sheep grazing, October-November
Dominant plant species	*Carex nigra*, *Agrostis capillaris*, *Dactylis glomerata*	*Securigera varia, Bromus erectus, Carex* sp.	*Carex montana, Sanguisorba officinalis, Agrostis capillaris*	*Bromus erectus*, *Trisetum flavescens*, *Salvia pratensis*

Table S2. Description of soil physicochemical parameters at the time of field sampling (i.e., not exposed to subsequent incubation in the laboratory) across the three studied seasons (spring, summer, autumn). For soil pH, we measured *N* = 3 per site and across seasons. For bulk density and gravimetric water content, we measured *N* = 5 per each site and season.

Site (block and elevation)	**Season**	**Soil pH**	**Bulk density (g cm^{-3})**	**Gravimetric water content (%)**
Chasseral (north high)	Spring	5.54 ± 0.67	0.60 ± 0.15	44.91 ± 3.94
	Summer		0.69 ± 0.11	36.10 ± 2.37
	Autumn		0.80 ± 0.20	36.70 ± 2.60
Le Landeron (north low)	Spring	7.91 ± 0.05	0.84 ± 0.13	24.47 ± 3.90
	Summer		0.95 ± 0.21	24.51 ± 1.93
	Autumn		0.89 ± 0.14	22.44 ± 1.07
Chasseron (south high)	Spring	5.10 ± 0.21	0.72 ± 0.12	44.00 ± 3.09
	Summer		0.68 ± 0.13	30.35 ± 2.86
	Autumn		0.61 ± 0.13	28.90 ± 4.55
Onnens (south low)	Spring	5.98 ± 0.25	1.19 ± 0.15	25.56 ± 1.30
	Summer		1.27 ± 0.05	15.29 ± 1.10
	Autumn		1.29 ± 0.16	20.35 ± 1.38

Table S3. Description of the experimental temperature regimes. Climatic data representative of high elevations was obtained from the weather station in Chasseral (47°07′54″N 7°03′16″E; 1596 m.a.s.l.), whereas for low elevation, we acquired data from the weather station in Neuchâtel (47°00′00″N 6°57′12″E; 485 m.a.s.l.). We retrieved air temperatures recorded at 2 m aboveground from the period 2015-2020 (source: Meteoswiss). Control temperatures were set as the average daily temperature over the reference period per elevation and season. To establish the extreme heat events for each elevation and season, we adopted the 99th percentile of daily temperatures across the reference period for spring (May-June), summer (July-August) and autumn (Spring-October). For both control and extreme heat temperature regimes, we included a diel light and temperature cycle (8h night/ 16h day), with a 6 °C-amplitude between night and day. C: Control temperature, EH: Extreme heat. The identity of the incubators (#1 to #4) containing each treatment combination is provided.

Elevation	Season	Temperature treatment	Average daily temperature (°C)	Daytime temperature (°C)	Nighttime temperature (°C)	Incubator ID
High	Spring	C	8.8	10.8	4.8	#3
		EH	20.5	22.5	16.5	#1
	Summer	C	13.5	15.5	9.5	#1
		EH	21.7	23.7	17.7	#4
	Autumn	C	7.3	9.3	3.3	#2
		EH	16.2	18.2	12.2	#4
Low	Spring	C	16.5	18.5	12.5	#2
		EH	26.6	28.6	22.6	#4
	Summer	C	21.2	23.2	17.2	#2
		EH	28.0	30.0	24.0	#3
	Autumn	C	13.6	15.6	9.6	#3
		EH	21.7	23.7	17.7	#1

Table S4. Total Collembola species abundances (*N* = 360) and vertical stratification of the species across the soil profile: epedaphic (surface-living), hemiedaphic (living in litter and upper soil layers) and euedaphic (permanently living in the soil). The sources for the identification of Collembola species were: Dunger & Schlitt (2011); Fjellberg (1998, 2007); Gisin (1960); Hopkin (2007); Thibaud *et al.* (2004). The vertical stratification of each Collembola species was extracted mainly from Gisin (1943), as well as Chauvat *et al.* (2014); Ferlian *et al.* (2015); Leinaas & Bleken (1983); Urbášek & Rusek (1994). The abundances of immature individuals that could not be assigned to a particular species are displayed at the bottom of the table.

Collembola species	**Family**	**Vertical stratification**	**Total abundance**
Folsomia quadrioculata	Isotomidae	Hemiedaphic	3502
Parisotoma notabilis	Isotomidae	Hemiedaphic	2867
Isotoma viridis	Isotomidae	Hemiedaphic	918
Isotomiella minor	Isotomidae	Euedaphic	890
Protaphorura pseudovanderdrifti	Onychiuridae	Euedaphic	863
Lepidocyrtus cyaneus	Entomobryidae	Hemiedaphic	820
Pseudosinella alba	Entomobryidae	Euedaphic	750
Lepidocyrtus lignorum	Entomobryidae	Epedaphic	461
Ceratophysella denticulata	Hypogastruridae	Epedaphic	351
Stenaphorura denisi	Tullbergiidae	Euedaphic	288
Sminthurinus signatus	Katiannidae	Hemiedaphic	251
Choreutinula inermis	Hypogastruridae	-	116
Sminthurinus aureus	Katiannidae	Epedaphic	48
Sphaeridia pumilis	Sminthurididae	Hemiedaphic	41
Neanura muscorum	Neanuridae	Hemiedaphic	20
Sminthurus viridis	Sminthurididae	Epedaphic	15
Orchesella flavescens	Orchesellidae	Epedaphic	5
Entomobrya multifasciata	Entomobryidae	Epedaphic	4
Pogonognathellus flavescens	Tomoceridae	Hemiedaphic	2
Heteromurus nitidus	Orchesellidae	Euedaphic	1
Immature individuals			
Isotomidae			397
Hypogastruridae			191
Entomobryidae			132
Symphypleona			7

Table S5. List of the controls incorporated in the amplicon sequencing pipeline.

Type of control	Description	Reference
Blank	Buffers from the extraction kit; added at the extraction phase	https://www.qiagen.com/us/products/discovery-and-translational-research/dna-rna-purification/dna-purification/microbial-dna/dneasy-powersoil-pro-kit
Negative	Elution buffer: buffer used to dilute samples, primers and in MasterMix	https://www.pacb.com/wp-content/uploads/Procedure-Checklist-%E2%80%93-Amplification-of-Full-Length-16S-Gene-with-Barcoded-Primers-for-Multiplexed-SMRTbell-Library-Preparation-and-Sequencing.pdf
Negative	MasterMix	https://www.pacb.com/wp-content/uploads/Procedure-Checklist-%E2%80%93-Amplification-of-Full-Length-16S-Gene-with-Barcoded-Primers-for-Multiplexed-SMRTbell-Library-Preparation-and-Sequencing.pdf
Positive	ATCC MSA-1010	https://www.atcc.org/products/msa-1010
Positive	ZymoBIOMICS Microbial Community Standard	https://zymoresearch.eu/products/zymobiomics-microbial-community-dna-standard-ii-log-distribution

Table S6. Ecological interpretation of the parameters from the joint species distribution models (jSDMs) used in our study. We tested the effects of season, elevation, treatment, and their three-way interactions, on Collembola and fungal species abundances. In the schematic visualization, green and orange lines represent positive and negative parameter estimates, respectively, while grey lines represent estimates that lack statistical support (i.e., blank fields in Fig. 3).

Parameter	Ecological interpretation	Schematic visualization
Intercept	Species abundances in the treatment combination set as the intercept: spring, at high elevation, in the control treatment.	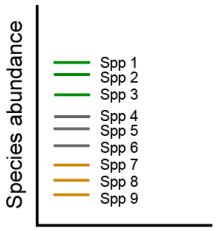
Summer	Shifts in abundance from spring to summer (relative to the intercept).	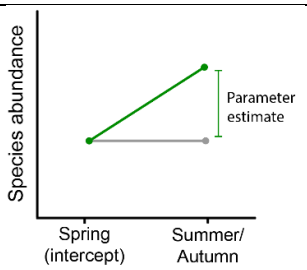
Autumn	Shifts in abundance from spring to autumn (relative to the intercept).	
Low elevation	Shifts in abundance from high to low elevation (relative to the intercept).	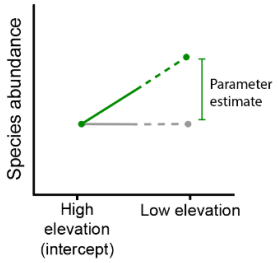
Summer x Low elevation	Given the seasonal abundance shifts as described above, it shows whether this effect is modulated by elevation (in control treatment).	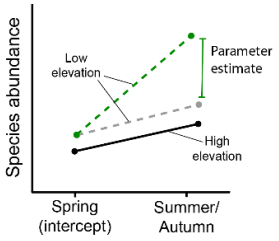
Autumn x Low elevation		
EH (extreme heat; including all the interactions involved)	Effect of the extreme heat event, compared to their corresponding reference level in the control treatment.	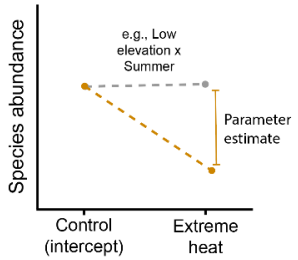

Table S7. Potential scale reduction factors for the parameters estimated in the joint species distribution models.

Model	Collembola					
Harvest	Baseline		Resistance		Recovery	
Parameter	Beta	Gamma	Beta	Gamma	Beta	Gamma
Min.	1.00	1.00	1.00	1.00	1.00	1.00
1st Qu.	1.00	1.00	1.00	1.00	1.00	1.00
Median	1.00	1.00	1.00	1.00	1.00	1.00
Mean	1.00	1.00	1.00	1.00	1.00	1.00
3rd Qu.	1.00	1.01	1.00	1.00	1.00	1.00
Max.	1.01	1.01	1.01	1.01	1.01	1.01
Model	Fungi (presence-absence)					
Harvest	Baseline		Resistance		Recovery	
Parameter	Beta	Gamma	Beta	Gamma	Beta	Gamma
Min.	1.00	1.00	1.00	1.00	1.00	1.00
1st Qu.	1.00	1.00	1.00	1.00	1.00	1.00
Median	1.00	1.00	1.00	1.00	1.00	1.00
Mean	1.00	1.00	1.00	1.00	1.00	1.00
3rd Qu.	1.00	1.00	1.00	1.00	1.00	1.00
Max.	1.02	1.01	1.02	1.01	1.01	1.01
Model	Fungi (abundance conditional on presence)					
Harvest	Baseline		Resistance		Recovery	
Parameter	Beta	Gamma	Beta	Gamma	Beta	Gamma
Min.	1.00	1.00	1.00	1.00	1.00	1.00
1st Qu.	1.00	1.00	1.00	1.00	1.00	1.00
Median	1.00	1.00	1.00	1.00	1.00	1.00
Mean	1.00	1.00	1.00	1.00	1.00	1.00
3rd Qu.	1.00	1.00	1.00	1.00	1.00	1.00
Max.	1.01	1.01	1.02	1.01	1.02	1.01
Model	Collembola-fungal models (only recovery)					
Parameter	Beta					
Treatment	Low spring	High spring	High summer	Low autumn	High autumn	
Min.	1.00	1.00	1.00	1.00	1.00	
1st Qu.	1.00	1.00	1.00	1.00	1.00	
Median	1.00	1.00	1.00	1.00	1.00	
Mean	1.00	1.00	1.00	1.00	1.00	
3rd Qu.	1.00	1.00	1.00	1.00	1.00	
Max.	1.02	1.02	1.02	1.08	1.04	

Table S8. Output of model used to compare the average daily soil temperature (measured at 3-5 cm depth) in the extreme heat events simulated in the lab, against the hottest days recorded in the field sites during the study period (*N* = 6 days, per each elevation and season combination). This analysis was conducted to evaluate the severity of our experimental treatments compared to the natural variability of heat extremes in the field sites. We fitted a linear mixed effect model with the R package nlme v.3.1-163 (Pinheiro et al., 2023), accounting for heterogeneity of residuals by taking the origin of the data (field or lab) as an offset term, due to the greater variance of the data collected from the field compared to the temperature data from the lab experiments. We note that the year in which the study took place (2022) was one of the warmest on record in the area, exceeding the norm of monthly mean temperature of May-October by 2.3-2.5 °C on average (relative to the 1990-2010 reference period; source Meteoswiss).

Average daily soil temperature (°C)						
Elevation	Season	Origin of data	Estimate	SE	*P*	Marginal/ Conditional R^2
High	Spring	Lab	19.60	0.33	0.060	0.993 / 0.998
		Field	18.02	0.24		
	Summer	Lab	20.75	0.33	0.087	
		Field	19.44	0.26		
	Autumn	Lab	15.72	0.33	**0.011**	
		Field	11.87	0.26		
Low	Spring	Lab	25.47	0.33	0.962	
		Field	25.49	0.24		
	Summer	Lab	27.23	0.33	0.322	
		Field	26.69	0.26		
	Autumn	Lab	21.03	0.33	**0.010**	
		Field	16.82	0.26		

Table S9. Output of the generalized linear mixed-effects model with negative binomial distribution used to evaluate the effect of the temperature treatments, modulated by elevation and season, on total Collembola abundances. Separate models were fit for each experimental harvest: baseline (harvest 1, before extreme heat), resistance (harvest 2, at the end of extreme heat) and recovery (harvest 3, five weeks after the end of extreme heat). Estimates, standard errors (SE), p-values (*P*) of the contrasts between temperature treatments, marginal and conditional R^2 (trigamma estimate) are provided. Significant p-values ($P < 0.05$) are highlighted in bold. Abbreviations of temperature treatment levels: C: Control temperature, EH: Extreme heat.

	Total Collembola abundances (log-scale)						
	Elevation	Season	Temperature treatment	Estimate	SE	*P*	Marginal/ Conditional R^2
Baseline (harvest 1)	High	Spring	C	3.86	0.21	0.651	0.263/0.305
			EH	3.76	0.21		
		Summer	C	3.71	0.22	0.356	
			EH	3.93	0.20		
		Autumn	C	3.18	0.25	0.218	
			EH	3.53	0.23		
	Low	Spring	C	3.28	0.25	0.949	
			EH	3.26	0.25		
		Summer	C	2.60	0.30	0.827	
			EH	2.68	0.29		
		Autumn	C	3.70	0.22	0.356	
			EH	3.92	0.20		
Resistance (harvest 2)	High	Spring	C	3.88	0.24	0.969	0.512/0.566
			EH	3.89	0.24		
		Summer	C	3.79	0.24	0.965	
			EH	3.80	0.24		
		Autumn	C	3.22	0.27	0.208	
			EH	3.56	0.25		
	Low	Spring	C	3.47	0.26	**<0.001**	
			EH	2.29	0.35		
		Summer	C	2.68	0.32	**0.007**	
			EH	1.19	0.52		
		Autumn	C	3.68	0.25	0.277	
			EH	3.40	0.27		
Recovery (harvest 3)	High	Spring	C	3.88	0.24	0.787	0.356/0.387
			EH	3.80	0.24		
		Summer	C	3.76	0.25	0.503	
			EH	3.55	0.26		
		Autumn	C	4.01	0.23	0.378	
			EH	3.77	0.24		
	Low	Spring	C	4.00	0.23	0.747	
			EH	3.91	0.24		
		Summer	C	3.09	0.29	**0.005**	
			EH	1.65	0.47		
		Autumn	C	4.14	0.22	0.323	
			EH	3.88	0.24		

Table S10. Output of the generalized linear mixed-effects model with negative binomial distribution used to evaluate the effect of the temperature treatments, modulated by elevation and season, on the total number of metabarcoding reads of saprotrophic fungi. Separate models were fit for each experimental harvest: baseline (harvest 1, before extreme heat), resistance (harvest 2, at the end of extreme heat) and recovery (harvest 3, five weeks after the end of extreme heat). Estimates, standard errors (SE), p-values (*P*) of the contrasts between temperature treatments, marginal and conditional R^2 (trigamma estimate) are provided. Significant p-values ($P < 0.05$) are highlighted in bold. Abbreviations of temperature treatment levels: C: Control temperature, EH: Extreme heat.

Number of reads of saprotrophic fungi (log-scale)							
	Elevation	Season	Temperature treatment	Estimate	SE	*P*	Marginal/ Conditional R^2
Baseline (harvest 1)	High	Spring	C	7.503	0.226	0.167	0.804/0.818
			EH	7.870	0.225		
		Summer	C	7.586	0.226	0.319	
			EH	7.322	0.225		
		Autumn	C	8.120	0.232	0.471	
			EH	7.925	0.226		
	Low	Spring	C	6.525	0.231	0.068	
			EH	7.013	0.239		
		Summer	C	6.974	0.225	0.730	
			EH	7.066	0.225		
		Autumn	C	7.401	0.225	0.562	
			EH	7.555	0.225		
Resistance (harvest 2)	High	Spring	C	7.223	0.322	0.581	0.720/0.820
			EH	7.347	0.322		
		Summer	C	7.148	0.322	0.503	
			EH	7.297	0.322		
		Autumn	C	7.712	0.322	0.843	
			EH	7.667	0.323		
	Low	Spring	C	6.680	0.327	0.680	
			EH	6.775	0.322		
		Summer	C	6.710	0.322	0.351	
			EH	6.502	0.322		
		Autumn	C	6.953	0.325	0.195	
			EH	6.652	0.322		
Recovery (harvest 3)	High	Spring	C	7.465	0.250	0.616	0.742/0.817
			EH	7.564	0.249		
		Summer	C	7.524	0.250	0.735	
			EH	7.591	0.249		
		Autumn	C	7.917	0.248	0.490	
			EH	8.054	0.252		
	Low	Spring	C	7.112	0.250	0.092	
			EH	6.775	0.249		
		Summer	C	7.320	0.249	0.089	
			EH	6.986	0.249		
		Autumn	C	7.511	0.253	**0.038**	
			EH	7.094	0.249		

Table S11. Output of the generalized linear mixed-effects model with negative binomial distribution used to evaluate the effect of the temperature treatments, modulated by elevation and season, on the total number of metabarcoding reads of pathogenic fungi. Separate models were fit for each experimental harvest: baseline (harvest 1, before extreme heat), resistance (harvest 2, at the end of extreme heat) and recovery (harvest 3, five weeks after the end of extreme heat). Estimates, standard errors (SE), p-values (*P*) of the contrasts between temperature treatments, marginal and conditional R^2 (trigamma estimate) are provided. Significant p-values ($P < 0.05$) are highlighted in bold. Abbreviations of temperature treatment levels: C: Control temperature, EH: Extreme heat.

	Number of reads of pathogenic fungi (log-scale)						
	Elevation	Season	Temperature treatment	Estimate	SE	*P*	Marginal/ Conditional R^2
Baseline (harvest 1)	High	Spring	C	5.845	0.277	0.606	0.649/0.689
			EH	5.997	0.278		
		Summer	C	6.211	0.277	0.544	
			EH	6.034	0.276		
		Autumn	C	6.327	0.280	0.136	
			EH	5.892	0.279		
	Low	Spring	C	6.417	0.280	0.945	
			EH	6.396	0.287		
		Summer	C	6.887	0.277	0.906	
			EH	6.922	0.276		
		Autumn	C	6.602	0.277	0.449	
			EH	6.377	0.280		
Resistance (harvest 2)	High	Spring	C	5.497	0.235	0.272	0.643/0.671
			EH	5.795	0.235		
		Summer	C	5.983	0.234	0.837	
			EH	5.928	0.234		
		Autumn	C	6.241	0.233	0.571	
			EH	6.394	0.236		
	Low	Spring	C	6.326	0.239	0.952	
			EH	6.342	0.235		
		Summer	C	6.781	0.235	0.560	
			EH	6.625	0.240		
		Autumn	C	6.301	0.234	0.774	
			EH	6.224	0.233		
Recovery (harvest 3)	High	Spring	C	6.557	0.199	0.151	0.656/0.659
			EH	6.172	0.193		
		Summer	C	6.195	0.198	0.541	
			EH	6.365	0.204		
		Autumn	C	6.782	0.193	0.114	
			EH	6.353	0.197		
	Low	Spring	C	6.383	0.194	0.241	
			EH	6.703	0.198		
		Summer	C	6.642	0.196	**0.002**	
			EH	7.471	0.196		
		Autumn	C	6.704	0.193	0.126	
			EH	7.110	0.193		

Table S12. Output of the network analysis evaluating differences between the Collembola-fungal association networks from extreme heat and control treatments. Z-scores and p-values were computed to establish whether the observed connectance differences were significantly greater or smaller compared to those from random networks generated with null models (1000 permutations for each network). Significant p-values ($P < 0.05$) are highlighted in bold. The connectance analysis was repeated separately for each fungal trophic group, on subsets of networks only made of either pathogens or saprotrophs. Connectance differences within the subsets of specific fungal groups are indicated; asterisks indicate the level of statistical significance (**$P < 0.01$). Whole network dissimilarity (WN) and its additive components are provided, based on Poisot *et al.* (2012) and Dormann *et al.* (2009): dissimilarity explained by the rewiring of associations among shared species (OS) and dissimilarity explained by differences in species composition between networks (ST). The percentages (%) of whole network dissimilarity explained by OS and ST components are shown. The observed association networks are displayed in Fig. S12.

Elevation	Season	Sign of associations	Connectance extreme heat	Connectance control	Connectance difference	z-score	*P*	Connectance differences within fungal groups	WN	OS	ST	% OS	% ST
High	Spring	Positive	0.082	0.099	-0.017	-0.475	0.635	None	0.719	0.234	0.484	32.6	67.4
		Negative	0.124	0.085	0.040	1.201	0.230	None	0.676	0.203	0.473	30.0	70.0
	Summer	Positive	0.076	0.044	0.032	0.233	0.815	None	0.967	0.283	0.683	29.3	70.7
		Negative	0.097	0.058	0.038	0.504	0.614	None	0.896	0.156	0.740	17.4	82.6
	Autumn	Positive	0.123	0.055	0.069	1.095	0.274	None	0.912	0.298	0.614	32.7	67.3
		Negative	0.075	0.055	0.020	0.299	0.765	None	0.880	0.361	0.518	41.1	58.9
Low	Spring	Positive	0.059	0.063	-0.005	-0.037	0.970	None	0.815	0.241	0.574	29.5	70.5
		Negative	0.136	0.061	0.075	2.958	**0.003**	Saprotroph**	0.770	0.287	0.483	37.3	62.7
	Autumn	Positive	0.078	0.032	0.046	1.383	0.167	None	0.891	0.145	0.745	16.3	83.7
		Negative	0.087	0.054	0.032	0.486	0.627	None	0.886	0.257	0.629	29.0	71.0

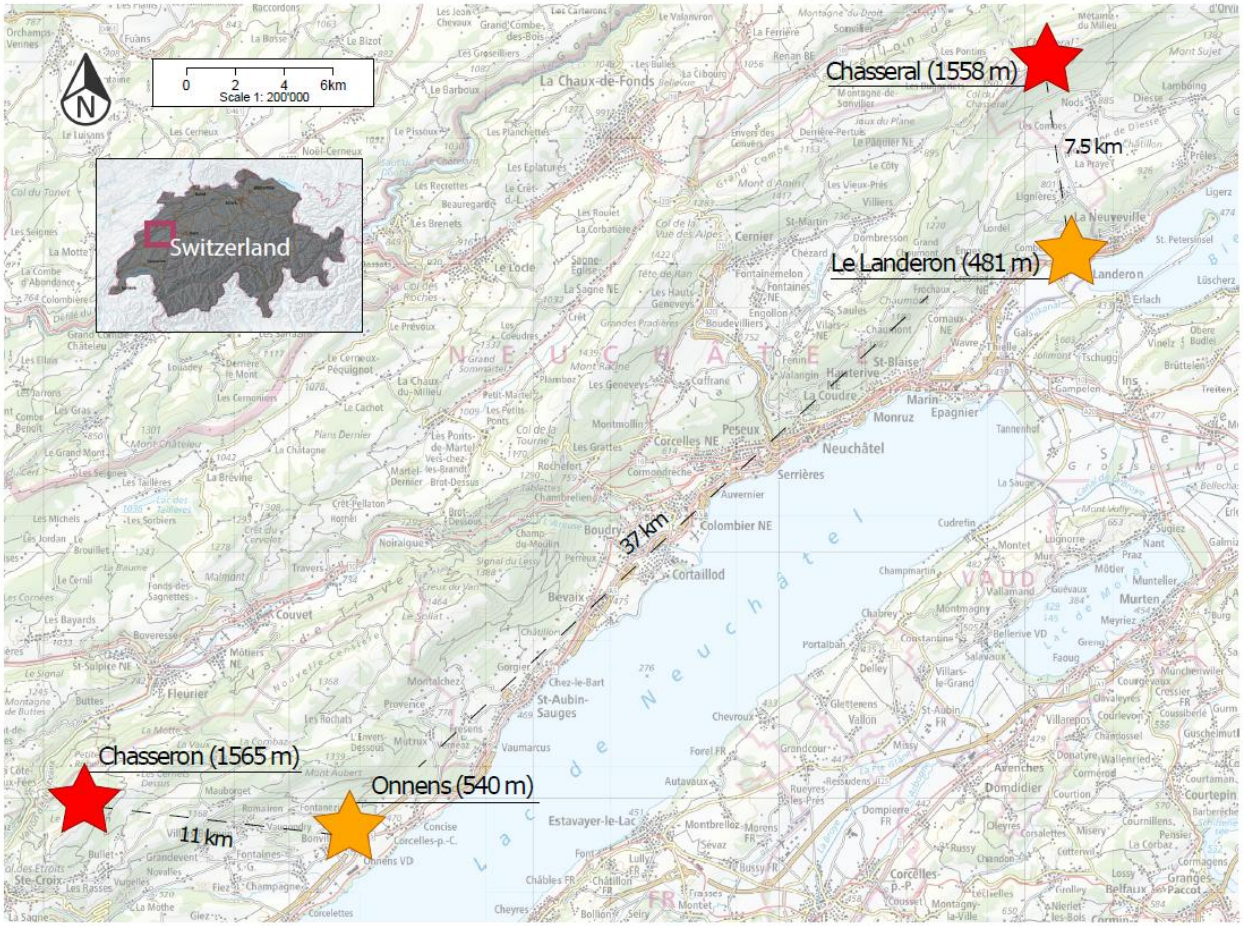

Fig. S1. Map of the study area showing the geographic position and elevation of the sampling sites, indicated with star signs. The shortest distance between sites of different blocks (north block: Chasseral and Le Landeron; south block: Chasseron and Onnens), as well as the distance between sites of the same block, are provided. Stars' colors indicate sites at different elevations: red: high elevation; orange: low elevation. Map adapted from https://map.geo.admin.ch.

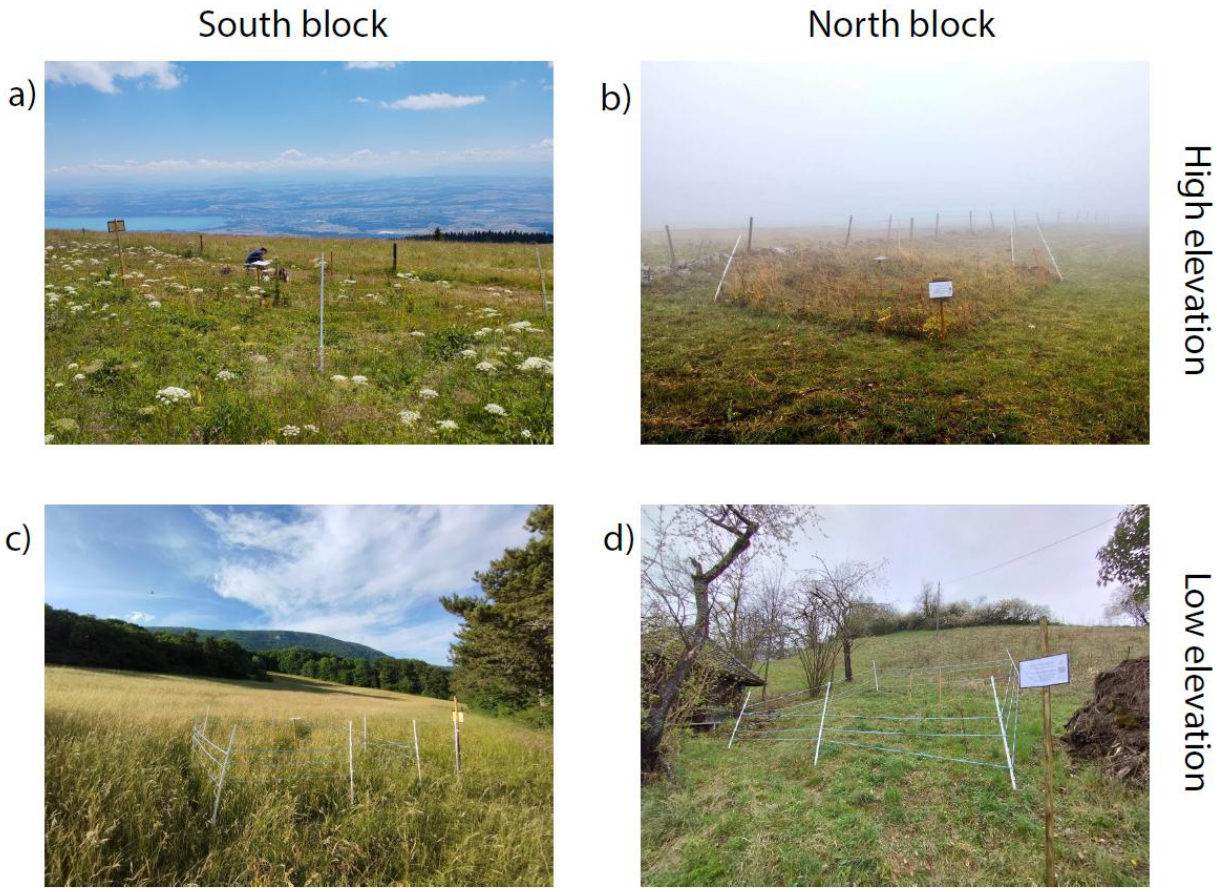

Fig. S2. Pictures of the field sites taken at various seasons: a) Chasseron (summer), b) Chasseral (autumn), c) Onnens (summer), d) Le Landeron (early spring, before the start of the experiments). The pictures are arranged in a grid, so that the rows indicate the elevation (high and low), and the columns show the block (south and north).

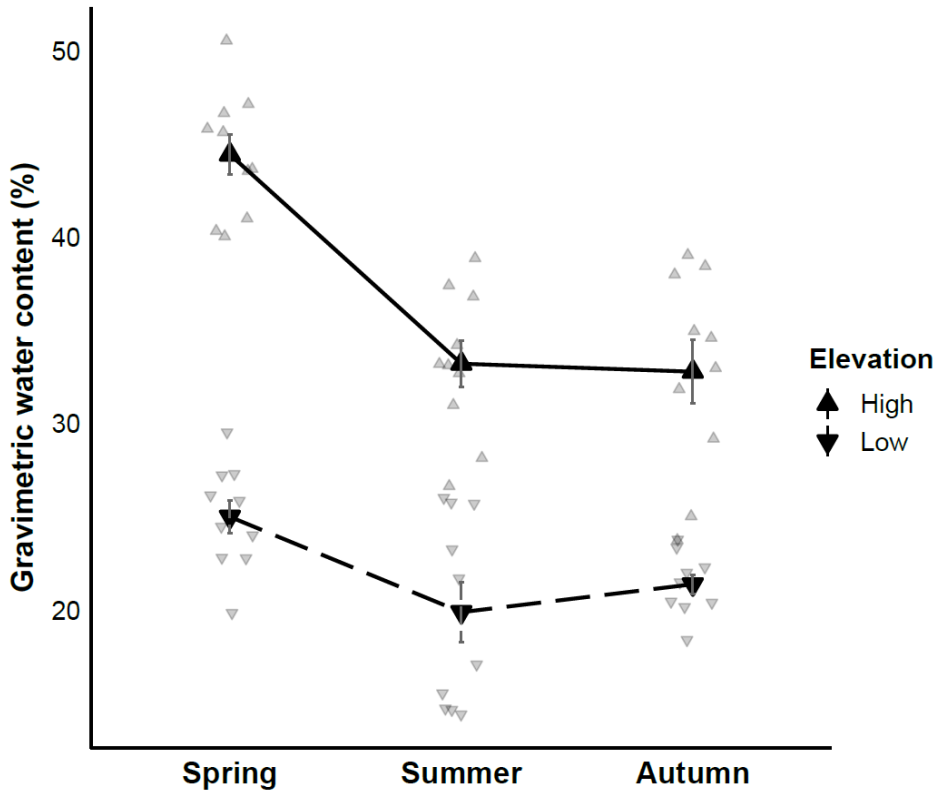

Fig. S3. Gravimetric soil water content, measured immediately after field sampling. Solid black points represent means, grey bars represent standard errors, and faded points are raw data (*N* = 10 per each elevation and season combination).

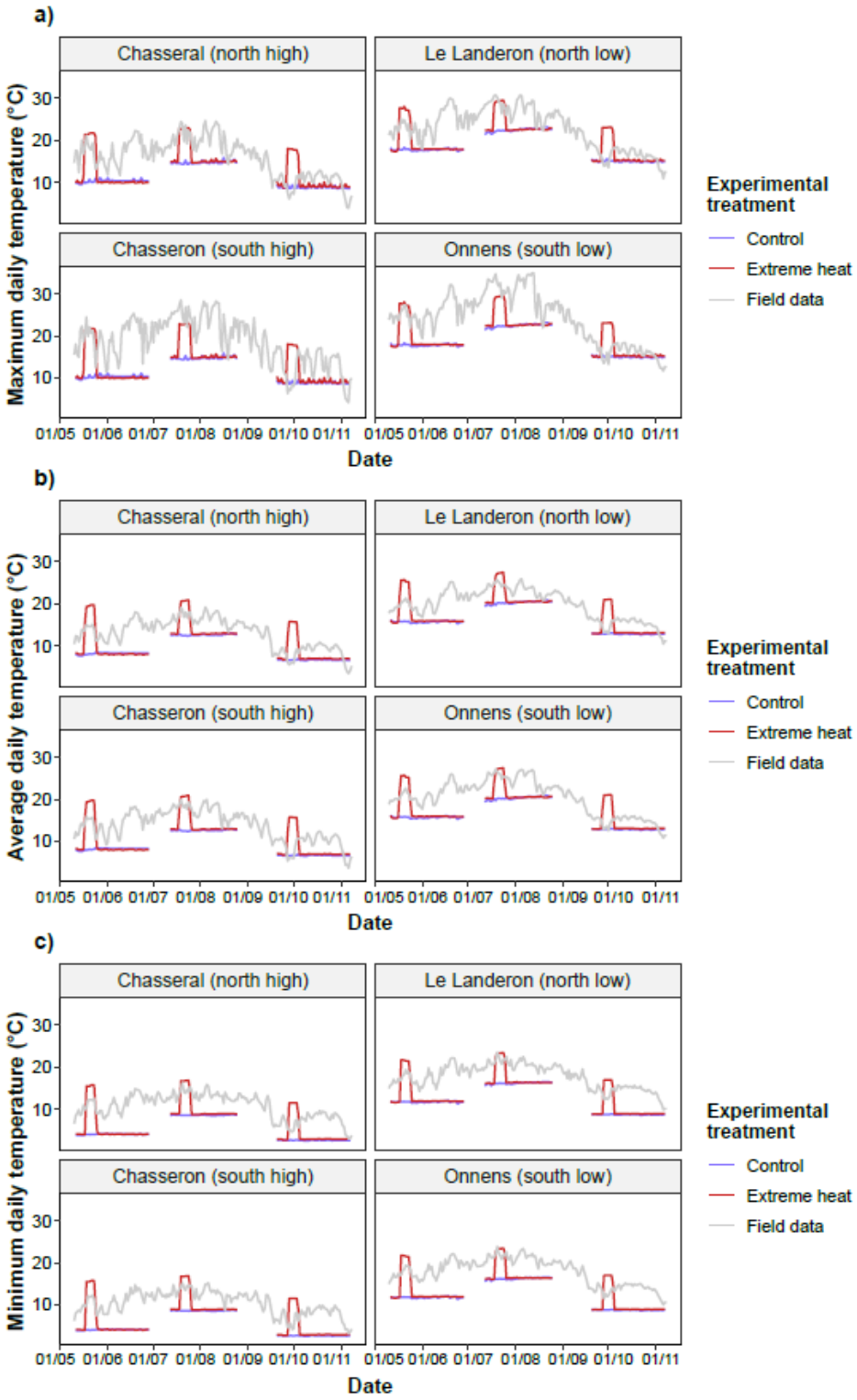

Fig. S4. Site-specific maximum (a), average (b) and minimum (c) daily soil temperatures at 5 cm depth, together with the daytime (a), average (b), and nighttime temperatures (c) recorded during the lab experiment, for both control (blue lines) and extreme heat treatments (red lines).

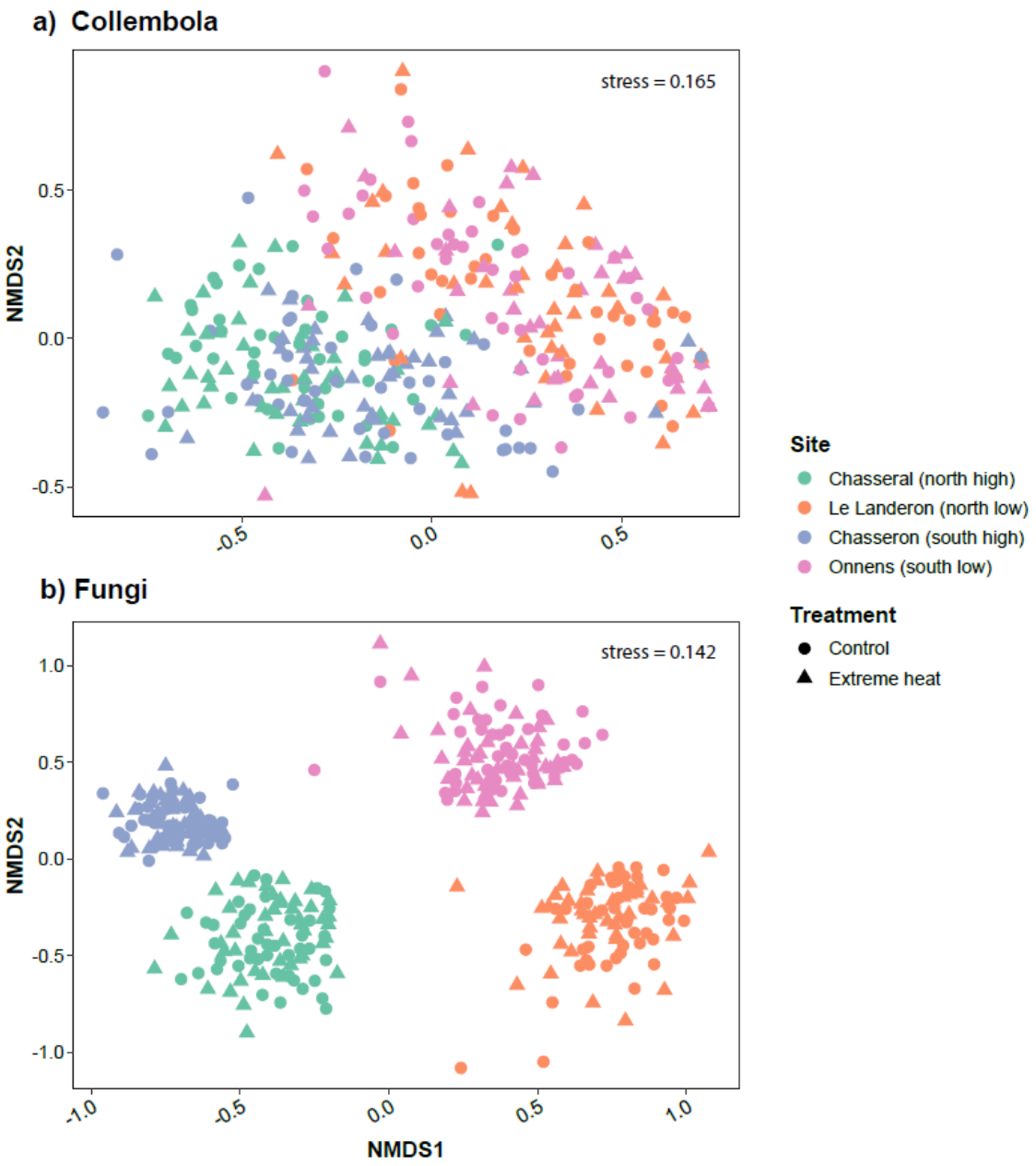

Fig. S5. Visualization of Collembola (a) and fungal communities (b) using non-metric multidimensional scaling (NDMS), implemented in the package *vegan* (version 2.6-4; Oksanen *et al.* 2022). Different colors indicate the sites: green: Chasseral; orange: Le Landeron; blue: Chasseron; pink: Onnens. The experimental treatments are shown with different shapes: round: control; triangle: extreme heat. We note that the first axis (NMDS1) mainly represents compositional differences between elevations (high/low), while the second axis (NMDS2) captures differences between the blocks (north/south). k=3 in both NDMS.

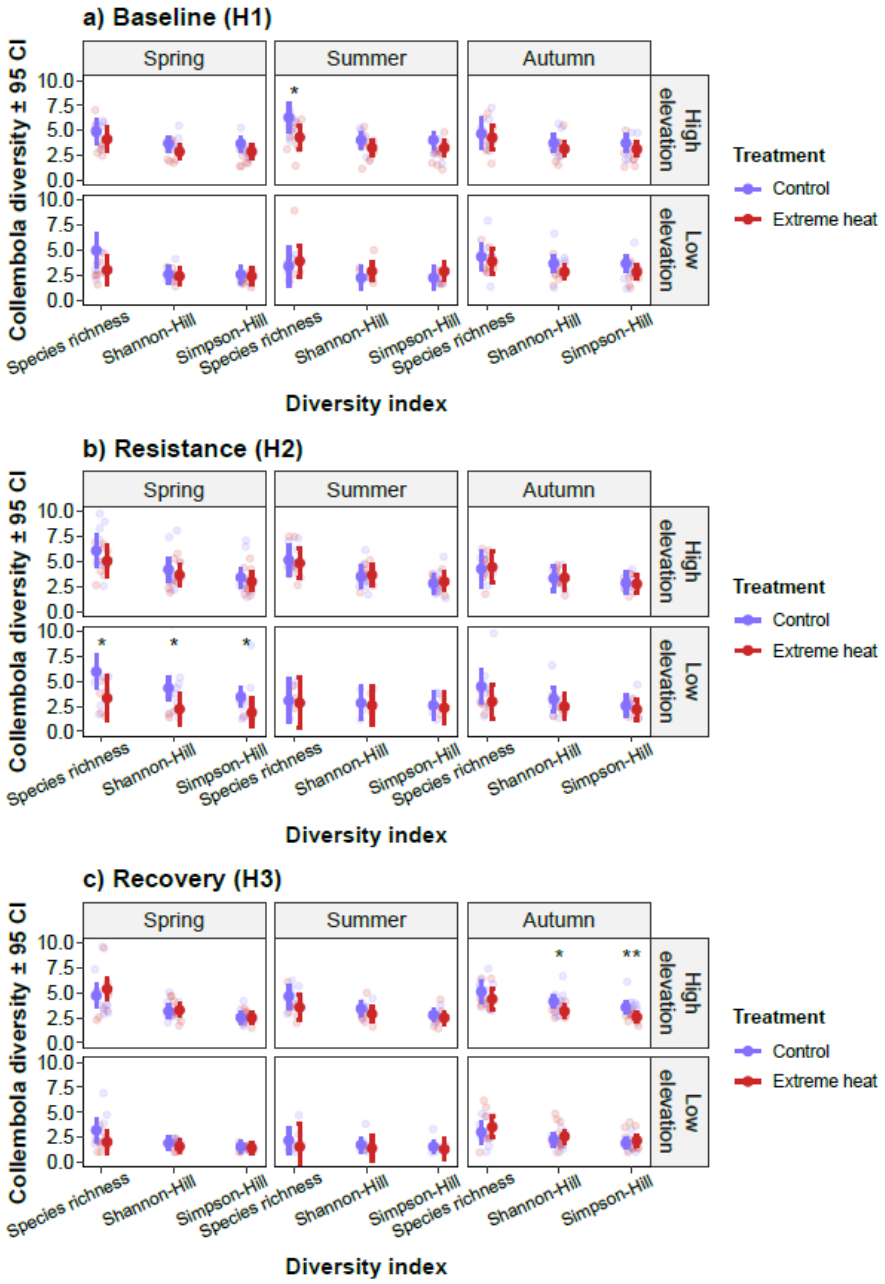

Fig. S6. Estimated marginal means (± 95 confidence intervals) of diversity profiles of Collembola communities, showing three indices calculated from various values of Hill number exponents (q): q = 0 (species richness), q = 1 (Shannon-Hill), q = 2 (Simpson-Hill). Lower values of the q exponent provide diversity estimates that give more leverage to rare species (e.g., species richness), while higher values give more leverage to dominant species (Roswell et al., 2021). Diversity profiles are shown for each experimental harvest separately: a) baseline or harvest 1 (H1; N = 97), b) resistance or harvest 2 (H2; N = 91), and c) recovery or harvest 3 (H3; N = 103). Colours indicate different experimental temperature treatments: blue: control; red: extreme heat. Stars show significant differences between treatments at each harvest: *P < 0.05, **P < 0.01.

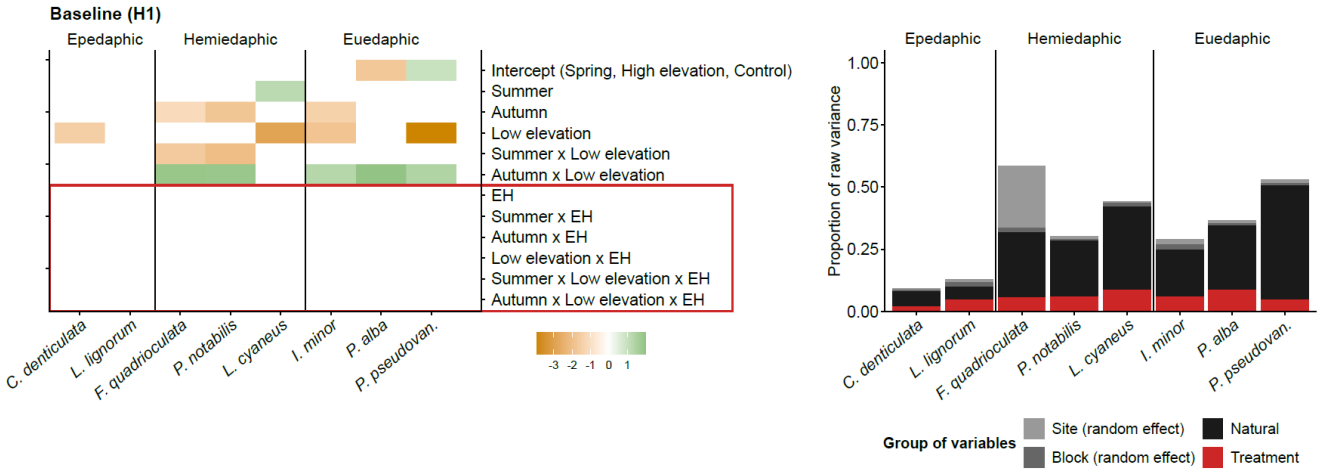

Fig. S7. Output of the joint species distribution models (jSDMs) fitted to investigate the responses of Collembola species abundances to season, elevation, treatment, and their three-way interactions, in the baseline response (i.e., harvest 1: H1; before the onset of the extreme heat events). Estimates from the beta parameters (left panels) show the responses of species abundances (x-axis) to each of the model parameters (y-axis). Green and orange colors indicate positive and negative responses with 95% posterior probability, respectively, while blank spaces denote responses that lacked statistical support. Species abundances at the intercept (spring, high elevation, control treatment) denote more abundant species in green, less abundant species in orange, and blank spaces indicating intermediate abundances. Parameters enclosed within the red area represent species responses to the experimental treatment (extreme heat: EH; see Table S6 for an ecological interpretation of the model parameters). The proportion of raw explained variance (right panels) is provided for different groups of variables: random effects (site and block), natural variables (season and elevation), and treatment (containing the variance explained by all parameters influenced by extreme heat, shown within the red area of the right panels). Collembola species are ordered according to their vertical stratification across the soil profile: epedaphic (surface-living), hemi-edaphic (living in litter and shallow soil layers), and euedaphic (permanently living in the soil).

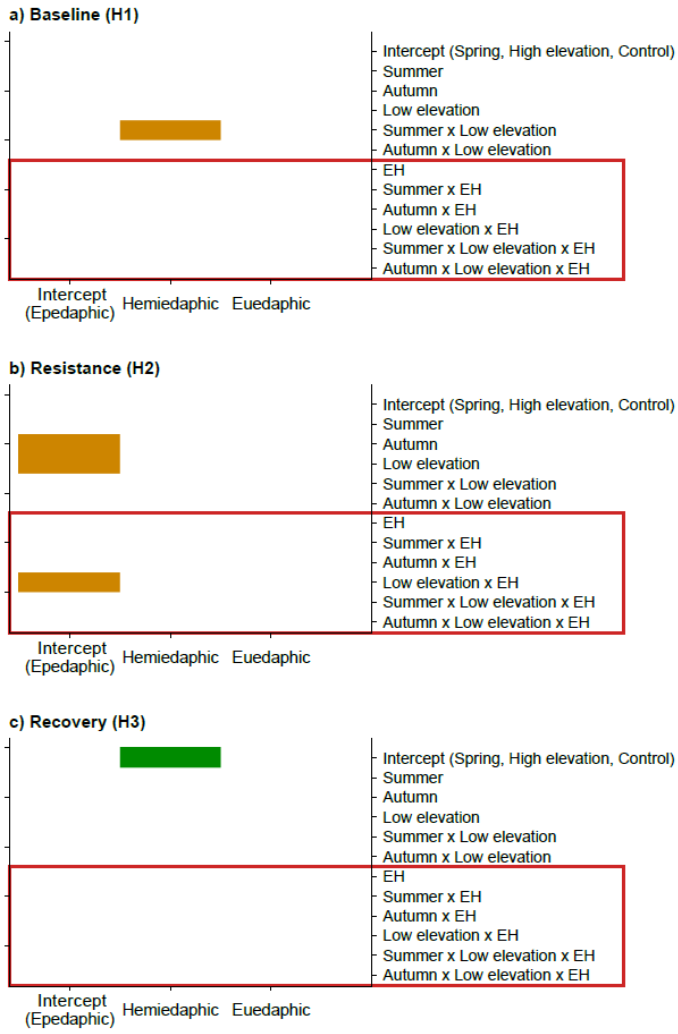

Fig. S8. Output of the joint species distribution models (jSDMs) fitted to investigate the responses of Collembola species abundances to season, elevation, treatment, and their three-way interactions, in the baseline (H1), resistance (H2) and recovery responses (H3). Estimates from the gamma parameters show whether species traits (i.e., vertical stratification; x-axis) mediate species abundance responses to each of the model parameters (y-axis). Three types of the vertical stratification of Collembola across the soil profile were investigated: epedaphic (surface-living), hemi-edaphic (living in litter and shallow soil layers), and euedaphic (permanently living in the soil). Green and orange colors indicate positive and negative responses with 95% posterior probability, respectively, while blank spaces denote responses that lacked statistical support. Parameter estimates at the intercepts (x-axis: epedaphic Collembola; y-axis: spring, high elevation, control treatment) denote higher overall abundances in green, lower overall abundances in orange, and blank spaces indicating intermediate abundances. The variation in species abundances explained by their vertical stratification (R_T^2; Ovaskainen *et al.* 2017) amounts to: 0.15 (baseline), 0.36 (resistance), 0.43 (recovery). Parameters enclosed within the red area represent species responses to the experimental treatment (extreme heat: EH; see Table S6 for an ecological interpretation of the model parameters).

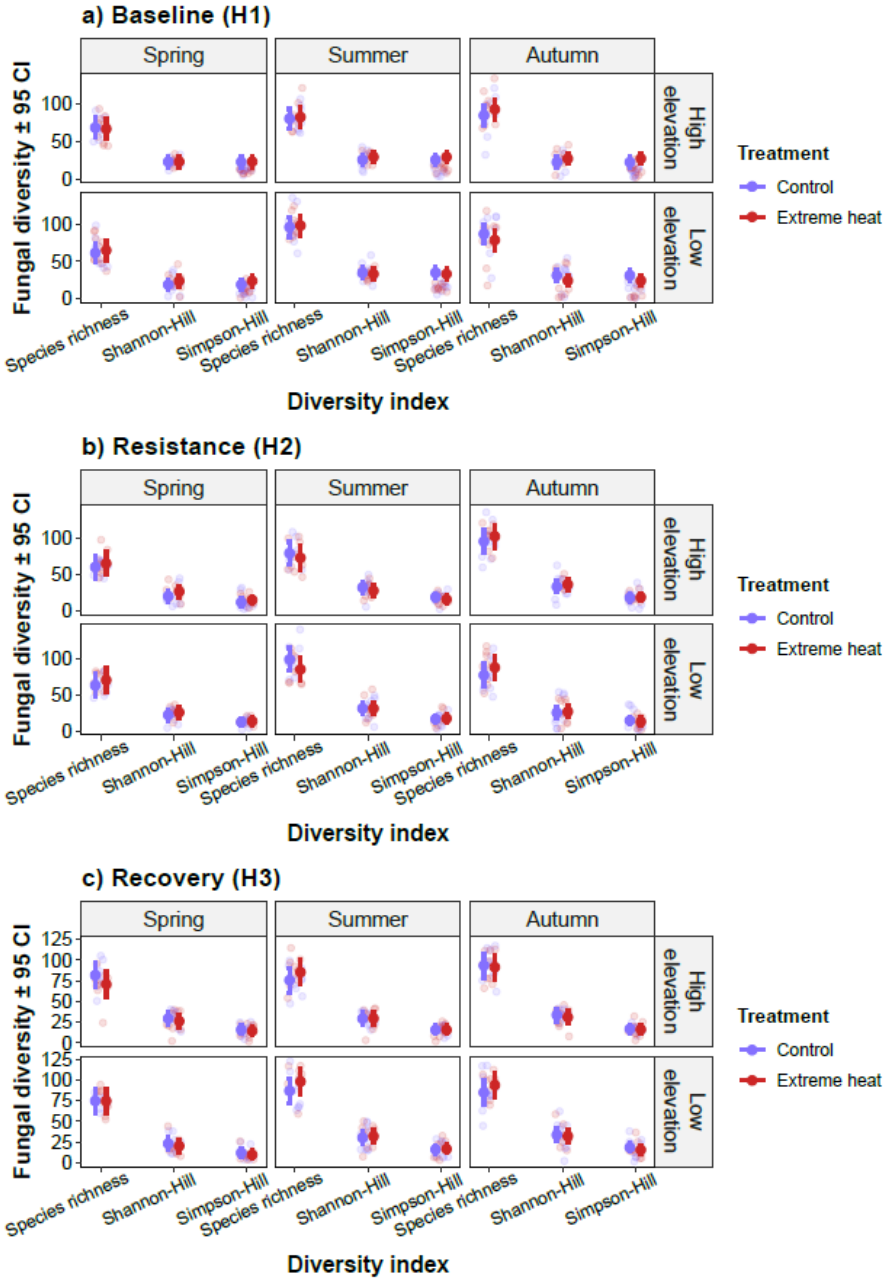

Fig. S9. Estimated marginal means (± 95 confidence intervals) of diversity profiles of fungal communities, showing three indices calculated from various values of Hill number exponents (*q*): *q* = 0 (species richness), *q* = 1 (Shannon-Hill), *q* = 2 (Simpson-Hill). Lower values of the *q* exponent provide diversity estimates that give more leverage to rare species (e.g., species richness), while higher values give more leverage to dominant species (Roswell et al., 2021). Diversity profiles are shown for each experimental harvest separately: a) baseline or harvest 1 (H1; *N* = 120), b) resistance or harvest 2 (H2; *N* = 120), and c) recovery or harvest 3 (H3; *N* = 120). Colours indicate different experimental temperature treatments: blue: control; red: extreme heat. The extreme heat treatment did not have significant effects on fungal diversity in any case.

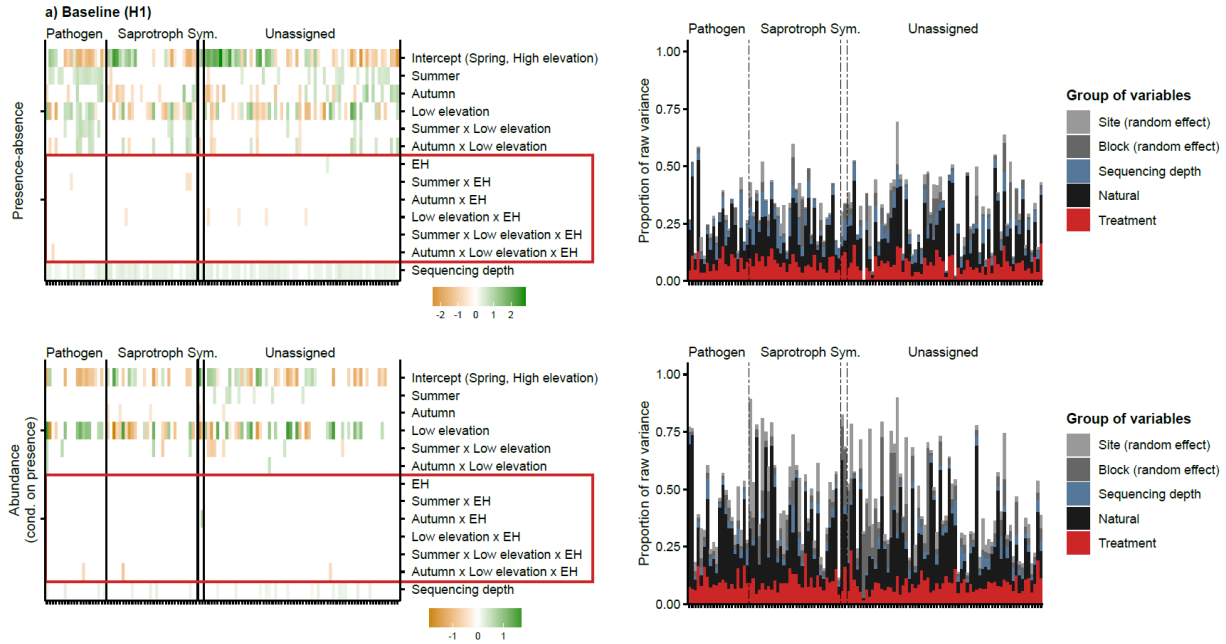

Fig. S10. Output of the joint species distribution models (jSDMs) fitted to investigate the responses of fungal species occurrences (panels above) and abundances (panels below) to season, elevation, treatment, and their three-way interactions, in the baseline response (i.e., harvest 1: H1; before the onset of the extreme heat events). Estimates from the beta parameters (left panels) show the species responses (x-axis) to each of the model parameters (y-axis). Green and orange colors indicate positive and negative responses with 95% posterior probability, respectively, while blank spaces denote responses that lacked statistical support. Species abundances at the intercept (spring, high elevation, control treatment) denote more abundant species in green, less abundant species in orange, and blank spaces indicating intermediate abundances. Parameters enclosed within the red area represent species responses to the experimental treatment (extreme heat: EH; see Table S6 for an ecological interpretation of the model parameters). The proportion of raw explained variance (right panels) is provided for different groups of variables: random effects (site and block), natural variables (season and elevation), and treatment (containing the variance explained by all parameters influenced by extreme heat, shown within the red area of the right panels). Fungal species are ordered according to their main trophic modes: pathogens, saprotrophs, symbionts, and unassigned fungi.

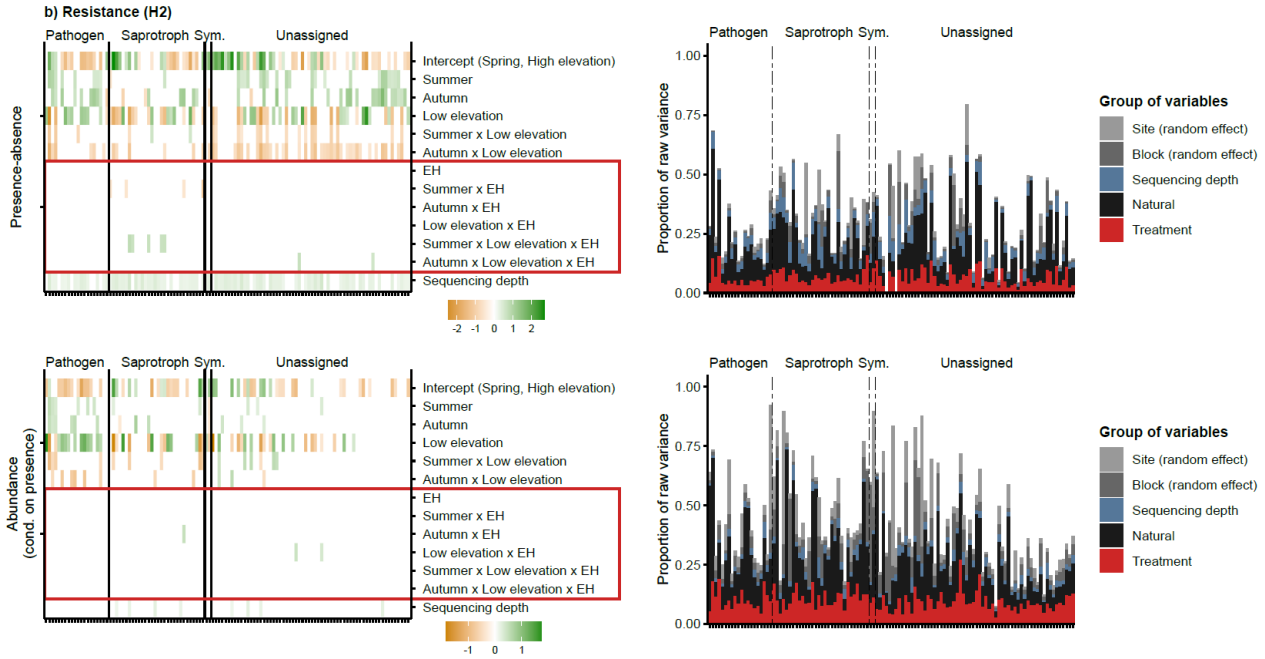

Fig. S11. Output of the joint species distribution models (jSDMs) fitted to investigate the responses of fungal species occurrences (panels above) and abundances (panels below) to season, elevation, treatment, and their three-way interactions, in the resistance response (i.e., harvest 2: H2; after the extreme heat events). Estimates from the beta parameters (left panels) show the species responses (x-axis) to each of the model parameters (y-axis). Green and orange colors indicate positive and negative responses with 95% posterior probability, respectively, while blank spaces denote responses that lacked statistical support. Species abundances at the intercept (spring, high elevation, control treatment) denote more abundant species in green, less abundant species in orange, and blank spaces indicating intermediate abundances. Parameters enclosed within the red area represent species responses to the experimental treatment (extreme heat: EH; see Table S6 for an ecological interpretation of the model parameters). The proportion of raw explained variance (right panels) is provided for different groups of variables: random effects (site and block), natural variables (season and elevation), and treatment (containing the variance explained by all parameters influenced by extreme heat, shown within the red area of the right panels). Fungal species are ordered according to their main trophic modes: pathogens, saprotrophs, symbionts, and unassigned fungi.

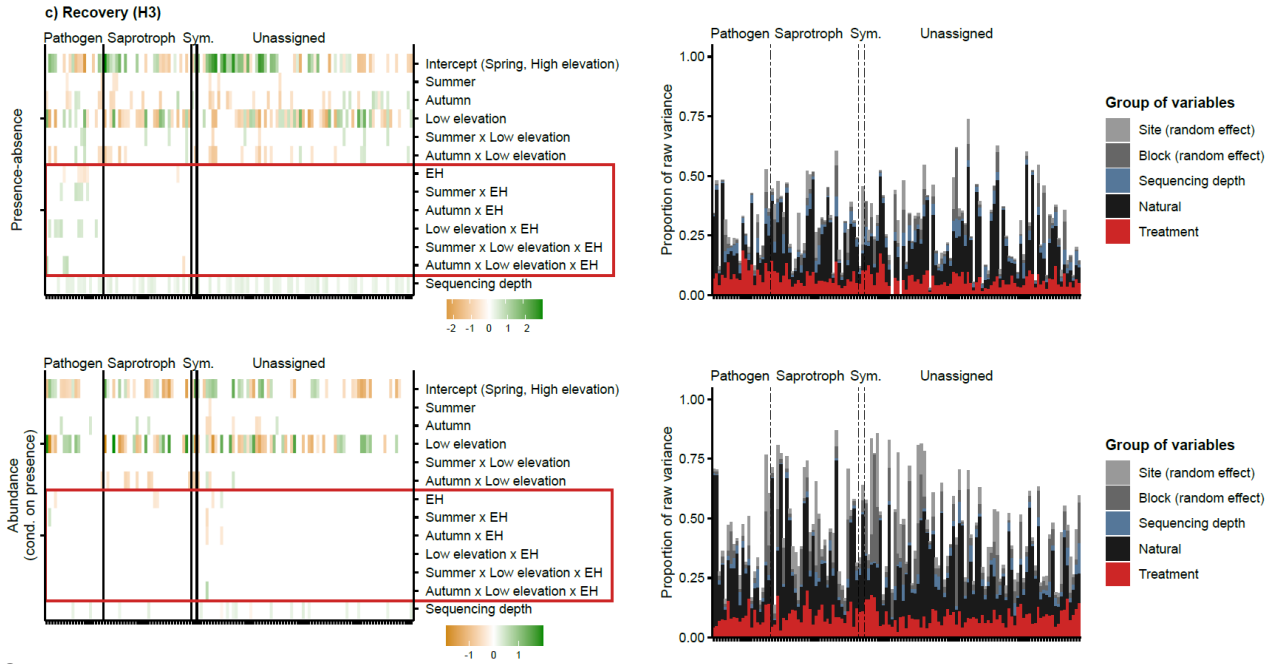

Fig. S12. Output of the joint species distribution models (jSDMs) fitted to investigate the responses of fungal species occurrences (panels above) and abundances (panels below) to season, elevation, treatment, and their three-way interactions, in the recovery response (i.e., harvest 3: H3; five weeks after the end of the extreme heat events). Estimates from the beta parameters (left panels) show the species responses (x-axis) to each of the model parameters (y-axis). Green and orange colors indicate positive and negative responses with 95% posterior probability, respectively, while blank spaces denote responses that lacked statistical support. Species abundances at the intercept (spring, high elevation, control treatment) denote more abundant species in green, less abundant species in orange, and blank spaces indicating intermediate abundances. Parameters enclosed within the red area represent species responses to the experimental treatment (extreme heat: EH; see Table S6 for an ecological interpretation of the model parameters). The proportion of raw explained variance (right panels) is provided for different groups of variables: random effects (site and block), natural variables (season and elevation), and treatment (containing the variance explained by all parameters influenced by extreme heat, shown within the red area of the right panels). Fungal species are ordered according to their main trophic modes: pathogens, saprotrophs, symbionts, and unassigned fungi.

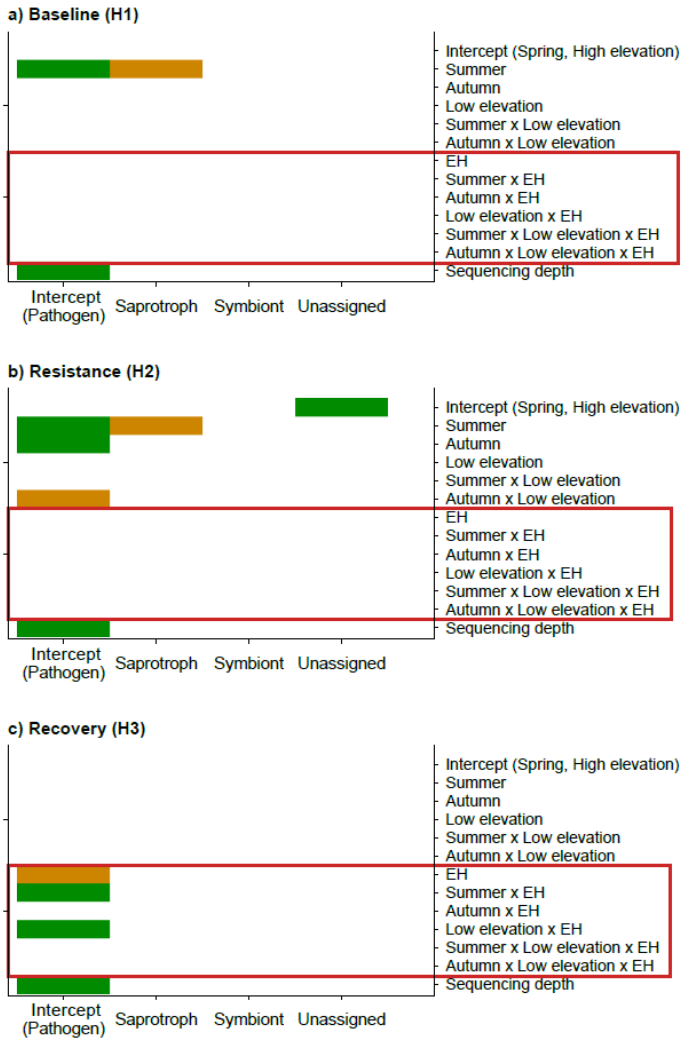

Fig. S13. Output of the joint species distribution models (jSDMs) fitted to investigate the responses of fungal species occurrences (i.e., presence-absence) to season, elevation, treatment, and their three-way interactions, in the baseline (H1), resistance (H2) and recovery responses (H3). Estimates from the gamma parameters show whether species traits (i.e., fungal trophic modes; x-axis) mediate species occurrence responses to each of the model parameters (y-axis). Three types of the fungal trophic modes were investigated: pathogens, saprotrophs and symbionts. Unassigned fungi represent the species for which a trophic mode could not be reliably determined. Green and orange colors indicate positive and negative responses with 95% posterior probability, respectively, while blank spaces denote responses that lacked statistical support. Parameter estimates at the intercepts (x-axis: pathogenic fungi; y-axis: spring, high elevation, control treatment) denote higher overall occurrences in green, lower overall occurrences in orange, and blank spaces indicating intermediate occurrences. The variation in species occurrences explained by their trophic modes (R_T^2; Ovaskainen *et al.* 2017) amounts to: 0.08 (baseline), 0.07 (resistance), 0.05 (recovery). Parameters enclosed within the red area represent species responses to the experimental treatment (extreme heat: EH; see Table S6 for an ecological interpretation of the model parameters).

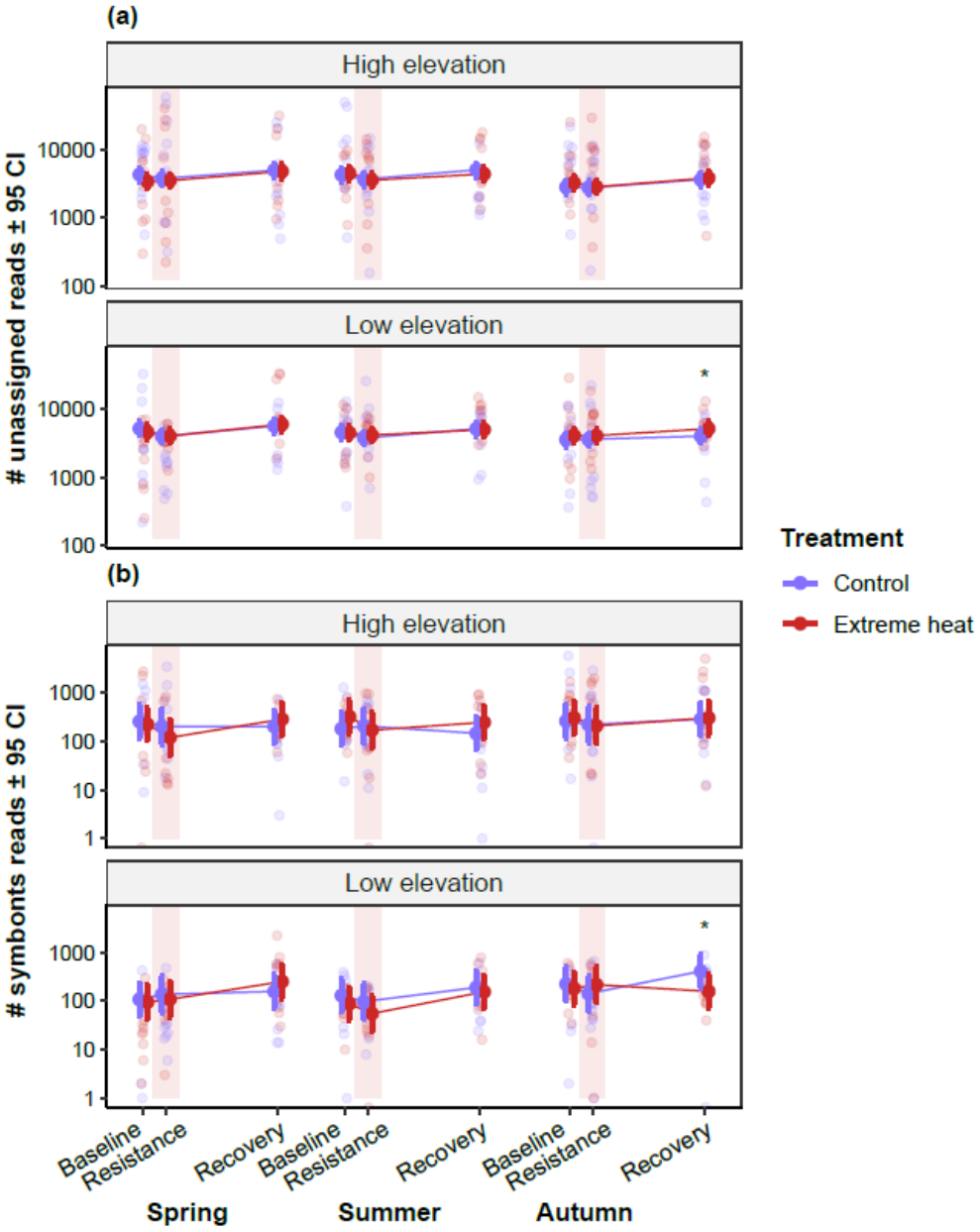

Fig. S14. Estimated marginal means (± 95 confidence intervals) of the number of reads (log-transformed) of unassigned (a; upper panel) and symbiotic fungi (b; lower panel) over the course of the experiments in spring, summer and autumn. The labels on the x-axis specify the different time points in which fungal metabarcoding reads were assessed during the experiment (i.e., harvests): baseline (harvest 1); resistance (harvest 2); recovery (harvest 3). The faded red areas represent the one-week extreme heat events. Colours indicate different experimental temperature treatments: blue: control; red: extreme heat. Stars show significant differences between treatments at each harvest: *$P < 0.05$.

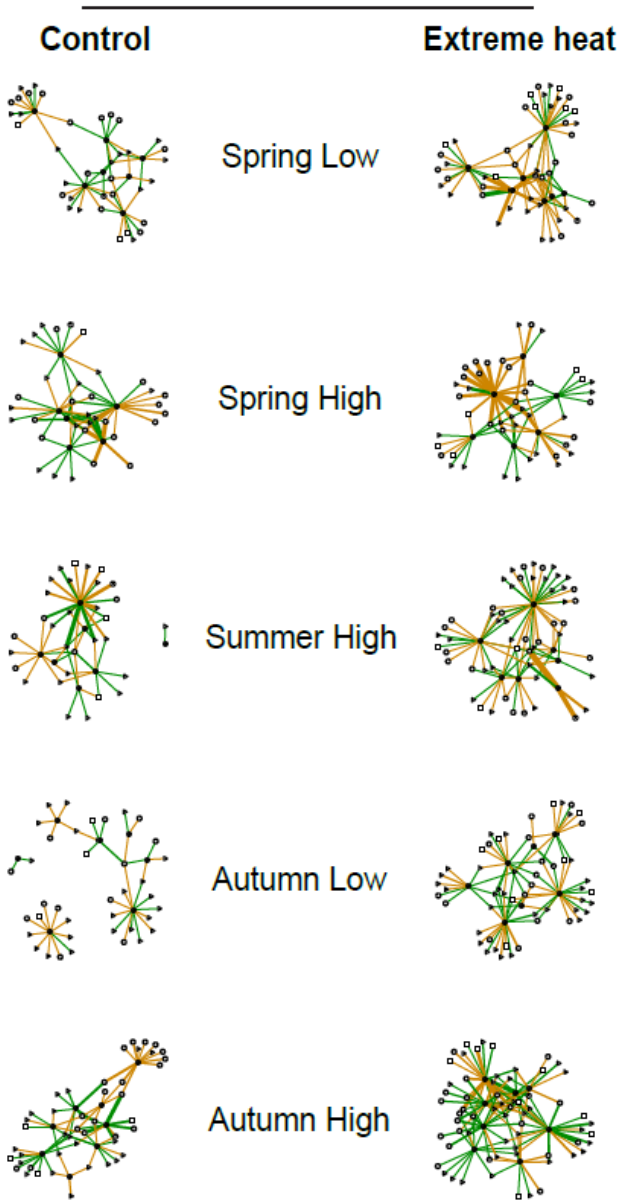

Fig. S15. Association networks of Collembola and fungi in the different spatiotemporal contexts (i.e., season and elevation) at the recovery response, separately for control (left column) and extreme heat treatments (right column). Positive associations are displayed with green colors and negative associations are shown with orange colors. The width of the links is proportional to the strength of the associations (i.e., parameter estimates of the Collembola-fungal jSDM). Black and white nodes denote Collembola and fungal species, respectively. Different node shapes represent various fungal trophic groups: saprotrophs (circle), pathogens (square), symbionts (pie), and unassigned fungi (triangle). Nodes without associations (i.e., degree = 0) are not displayed. A high-resolution version of the figure is available at the data repository (*Data from: Belowground Communities in Lowlands Are Less Stable to Climate Extremes across Seasons*, 2025).

SI References

Chauvat, M., Perez, G., & Ponge, J. F. (2014). Foraging patterns of soil springtails are impacted by food resources. *Applied Soil Ecology*, *82*, 72–77. https://doi.org/10.1016/j.apsoil.2014.05.012

Data from: Belowground communities in lowlands are less stable to climate extremes across seasons. (2025). [Dataset]. Figshare Repository. https://doi.org/10.6084/m9.figshare.26142490

Dormann, C. F., Frund, J., Bluthgen, N., & Gruber, B. (2009). Indices, Graphs and Null Models: Analyzing Bipartite Ecological Networks. *The Open Ecology Journal*, *2*(1), 7–24. https://doi.org/10.2174/1874213000902010007

Dunger, W., & Schlitt, B. (2011). Synopses on Palaearctic Collembola – Tullbergiidae. *Soil Organisms*, *83*(1), Article 1.

Ferlian, O., Klarner, B., Langeneckert, A. E., & Scheu, S. (2015). Trophic niche differentiation and utilisation of food resources in collembolans based on complementary analyses of fatty acids and stable isotopes. *Soil Biology and Biochemistry*, *82*, 28–35. https://doi.org/10.1016/j.soilbio.2014.12.012

Fjellberg, A. (1998). *The Collembola of Fennoscandia and Denmark, Part I: Poduromorpha* (Vol. 35, p. 184). Brill. https://brill.com/display/title/6555

Fjellberg, A. (2007). *The Collembola of Fennoscandia and Denmark, Part II: Entomobryomorpha and Symphypleona* (Vol. 42). Brill. https://brill.com/display/title/14147

Gisin, H. (1960). *Collembolenfauna Europas*. Museum D'Histoire Naturelle Genève.

Gisin, H. F. (1943). *Oekologie und Lebensgemeinschaften der Collembolen im schweizerischen Exkursionsgebiet Basels*. Kundig. https://books.google.ch/books?id=m5HFzQEACAAJ

Hopkin, S. P. (2007). *A Key to the Collembola (springtails) of Britain and Ireland*. FSC.

Leinaas, H. P., & Bleken, E. (1983). Egg diapause and demographic strategy in *Lepidocyrtus lignorum* Fabricius (Collembola; Entomobryidae). *Oecologia*, *58*(2), 194–199.

Oksanen, J., Simpson, G., Blanchet, F., Kindt, R., Legendre, P., Minchin, P., O'Hara, R., Solymos, P., Stevens, M., Szoecs, E., Wagner, H., Barbour, M., Bedward, M., Bolker, B., Borcard, D., Carvalho, G., Chirico, M., De Caceres, M., Durand, S., … Weedon, J. (2022). *vegan: Community Ecology Package* [Computer software]. https://cran.r-project.org/package=vegan

Ovaskainen, O., Tikhonov, G., Norberg, A., Guillaume Blanchet, F., Duan, L., Dunson, D., Roslin, T., & Abrego, N. (2017). How to make more out of community data? A conceptual framework and its implementation as models and software. *Ecology Letters*, *20*(5), 561–576. https://doi.org/10.1111/ele.12757

Pinheiro, J., Bates, B., & R Core Team. (2023). *nlme: Linear and Nonlinear Mixed Effects Models* [Computer software]. https://cran.r-project.org/package=nlme

Poisot, T., Canard, E., Mouillot, D., Mouquet, N., & Gravel, D. (2012). The dissimilarity of species interaction networks. *Ecology Letters*, *15*(12), 1353–1361. https://doi.org/10.1111/ele.12002

Roswell, M., Dushoff, J., & Winfree, R. (2021). A conceptual guide to measuring species diversity. *Oikos*, *130*(3), 321–338. https://doi.org/10.1111/oik.07202

Thibaud, J.-M., Schulz, H.-J., & da Gama, M. M. (2004). *Synopses on Palaearctic Collembola, Volume IV: Hypogastruridae* (Vol. 75). https://www.nhbs.com/en/synopses-on-palaearctic-collembola-volume-4-hypogastruridae-book

Urbášek, F., & Rusek, J. (1994). Activity of digestive enzymes in seven species of Collembola (Insecta: Entognatha). *Pedobiologia*, *38*(5), 400–406. https://doi.org/10.1016/s0031-4056(24)00143-4